



Simulating Bark Beetle Outbreak Dynamics and their Influence on Carbon Balance Estimates with ORCHIDEE r7791

Guillaume Marie^{1*}, Jina Jeong^{2*}, Hervé Jactel³, Gunnar Petter⁴, Maxime Cailleret⁵, Matthew J.
5 McGrath¹, Vladislav Bastrikov⁶, Josefine Ghattas⁷, Bertrand Guenet⁸, Anne-Sofie Lansø⁹, Kim
Naudts¹¹, Aude Valade¹⁰, Chao Yue¹², Sebastiaan Luyssaert²

¹ Laboratoire des Sciences du Climat et de l'Environnement, CEA CNRS UVSQ UP Saclay, 91191 Orme des
Merisiers, Gif-sur-Yvette, France

10 ² Faculty of Science, A-LIFE, Vrije Universiteit Amsterdam, 1081 HV Amsterdam, the Netherlands

³ INRAE, University of Bordeaux, UMR Biogeco, 33612 Cestas, France

⁴ ETH Zürich, Department of Environmental Systems Science, Forest Ecology, 8092 Zürich, Switzerland

⁵ INRAE, Aix-Marseille Univ, UMR RECOVER, 13182 Aix-en-Provence, France

⁶ Science Partner, France

15 ⁷ Institut Pierre-Simon Laplace – Sciences du climat (IPSL), 75105 Jussieu, France

⁸ Laboratoire de Géologie, Ecole Normale Supérieure, CNRS, PSL Research University, IPSL, 75005 Paris, France

⁹ Department of Environmental Science, Aarhus Universitet, Frederiksborgvej 399, 4000 Roskilde, Denmark

¹⁰ Eco & Sols, Univ Montpellier, CIRAD, INRAE, 34060 Institut Agro, IRD, Montpellier, France

¹¹ Department of Earth Sciences, Vrije Universiteit Amsterdam, 1081 HV Amsterdam, the Netherlands

20 ¹² State Key Laboratory of Soil Erosion and Dryland Farming on the Loess Plateau, Northwest A & F University,
Yangling, Shaanxi, China

* These authors contributed equally to this study

25 **Corresponding author:** Guillaume Marie, guillaume.marie@lscce.ipsl.fr, Jina Jeong, j.jeong@vu.nl, Sebastiaan
Luyssaert, s.luyssaert@vu.nl

Abstract: New (a)biotic conditions, resulting from climate change, are expected to change disturbance dynamics,
e.g., wind throw, forest fires and insect outbreaks, and their interactions. Unprecedented natural disturbance
30 dynamics might alter the capability of forest ecosystems to buffer atmospheric CO₂ increases in the atmosphere,
even leading to the risk that forests transform from sinks into sources of CO₂. This study aims to enhance the
capability of the ORCHIDEE land surface model to study the impacts of climate change on bark beetle dynamics
and subsequent effects on forest functioning. The bark beetle outbreak model is based on previous work by Temperli
et al. 2013 for the LandClim landscape model. The new implementation of this model in ORCHIDEE r7791
35 accounts for the following differences between ORCHIDEE and LandClim: (1) the coarser spatial resolution of



ORCHIDEE, (2) the higher temporal resolution of ORCHIDEE, and (3) the pre-existing process representation of wind throw, drought, and forest structure in ORCHIDEE. Qualitative evaluation demonstrated the model's ability to simulate a wide range of observed post-disturbance forest dynamics: (1) resistance to bark beetle infestation even in the presence of windthrow events; (2) slow transition (3-7 years) from an endemic into an epidemic bark beetle population following medium intensity window events at cold locations; and (3) fast transition (1-3 years) from endemic to epidemic triggered by strong windthrow events. Although all simulated sites eventually recovered from disturbances, the time needed to recover varied from 5 to 10 years depending on the disturbance dynamics. In addition to enhancing the functionality of the ORCHIDEE model, the new bark beetle model represents a fundamental change in the way mortality is simulated as it replaces a framework in which mortality is conceived as a continuous process by one in which mortality is represented by abrupt events. Changing the mortality framework provided new insights into carbon balance estimates, showing the risk of overestimating the short-term sequestration potential under the commonly used continuous mortality framework.

Table 1: List of abbreviations

Symbol	Description	Units
Act_{y-1}	Bark beetle activity index in the previous year	unitless
Age	Age of the dominant spruce trees in a spatial entity	year
BA	Basal area of trees in a spatial entity	m ²
Bdb	Dead biomass from bark beetle attack	t/ha
Bdw	Dead biomass from windthrow	t/ha
Binf	Living biomass infested by bark beetles	t/ha
Bmax	Maximum potential biomass of a European Forest	t/ha
Bt	Actual total biomass of spruce forest	t/ha
Bw	Actual woody biomass of spruce forest	t/ha
BPI	Bark beetle pressure index	unitless
D	Distance between two patches	m
Dw	Maximum distance for which windthrow can affect surrounding patches	m
Cbp	Spatial scaling coefficient	unitless
Cst	Temporal scaling coefficient	unitless
Frac	Area fraction within a pixel	unitless
G	Bark beetle generation index	unitless



K	Thermal sum of degrees days for one bark beetle generation	°C/day
$Litw$	Woody biomass left on the forest floor	t/ha
$Litt$	Litter to stand biomass ratio at which S_{iw} is maximum	unitless
m	Midpoint of the function for degree days	unitless
r	Logistic growth rate	unitless
S_i	Susceptibility index [0,1]	unitless
S_{ir}	Susceptibility index for stand density [0,1]	unitless
S_{id}	Susceptibility index for tree health [0,1]	unitless
S_{is}	Susceptibility index for spruce abundance [0,1]	unitless
S_{iw}	Susceptibility index for tree mortality from windthrow [0,1]	unitless
$SumT_{eff}$	Sum of effective temperature for bark beetle reproduction	°C/day
W_r	Weight for stand density index	unitless
W_d	Weight for drought index	unitless
W_s	Weight for spruce abundance	unitless
W_w	Weight for windthrow damage	unitless

1. Introduction

- 50 Considerable uncertainties remain about the magnitude of Earth system impacts from all future climate change scenarios, even the most modest (Pörtner et al., 2022). One major source of uncertainty is that future climate will likely bring new abiotic constraints through the co-occurrence of multiple connected hazards, e.g., “hotter droughts”, which are droughts combined with heat waves (Allen et al., 2015; Zscheischler et al., 2018), but also new biotic conditions from interacting natural and anthropogenic disturbances, e.g., insect outbreaks following wind throw or
- 55 forest fires (Seidl et al., 2017). Unprecedented natural disturbance dynamics might alter biogeochemical cycles specifically the capability of forest ecosystems to buffer the CO₂ increase in the atmosphere (Hicke et al., 2012; Seidl et al., 2014) and the risk that forests are transformed from sinks into sources of CO₂ (Kurz et al., 2008). The magnitude of such alteration, however, remains uncertain principally due to the lack of impact studies that include disturbance regime shifts at global scale (Seidl et al., 2011).
- 60 Land surface models are used to study the relationships between climate change and the biogeochemical cycles of carbon, water, and nitrogen (Cox et al., 2000; Ciais et al., 2005; Friedlingstein et al., 2006; Zaehle and Dalmonech, 2011; Luysaert et al., 2018). Many of these models use background mortality to obtain an equilibrium in their biomass pools. Moreover, the classic approach of studying forest dynamics, which assumes steady-state conditions over long periods of time, may not be suitable for assessing the impacts of disturbances on shorter time scales under a climate



65 of accelerating changes. This is important because such disturbances can have significant impacts on ecosystem services, such as water regulation, carbon sequestration, and biodiversity (Quillet et al., 2010).

Mechanistic approaches that account for a variety of mortality drivers, such as age, size, competition, climate, and disturbances, are now being used to simulate forest dynamics more accurately (Migliavacca et al., 2021). For example, the ORCHIDEE model considers mortality induced by interspecific competition for light in addition to background mortality. Incorporating a more mechanistic view on mortality is important for improving our understanding of the impacts of climate change on forest dynamics and the provision of ecosystem services.

70 Land surface models also face the challenge of better describing mortality particularly when it comes to ecosystem responses to “cascading disturbances”, where legacy effects from one disturbance affect the next (Zscheischler et al., 2018; Buma, 2015). Biotic disturbances, such as bark beetle outbreaks, strongly depend on previous disturbances as their infestation capabilities are higher when tree vitality is low, for example following drought or storm events (Seidl et al., 2018). This illustrates how interactions between biotic and abiotic disturbances can have significant effects on ecosystem dynamics and must be incorporated into land surface models to improve our understanding of the impacts of climate change on forest dynamics (Temperli et al., 2013; Seidl et al., 2011). While progress has been made towards including abrupt mortality from individual disturbance types such as wildfire (Yue et al., 2014; Lasslop et al., 2014; Migliavacca et al., 2013), windthrow (Chen et al., 2018) and drought (Yao et al., 2022), the interaction of biotic and abiotic disturbances remains both a knowledge and modeling gap (Kautz et al., 2018).

85 Bark beetle outbreaks are becoming increasingly important biotic disturbances across the world (Seidl et al., 2018; Bentz et al., 2010). A massive bark beetle outbreak in the Canadian and American Rocky Mountains damaged more than 90% of the Engelmann spruce trees across ~325,000 ha from 2005 to 2017 (Andrus et al., 2020). Damage caused by the spruce bark beetle *Ips typographus* is also on the rise in Europe, and is responsible for as much as 8% of all tree mortality due to natural disturbances in Europe between 1850 and 2000 (Hlásny et al., 2021). In particular, a strong link between previous windthrow and bark beetle outbreaks has been reported (Pasztor et al., 2014; Mezei et al., 2017). These observations justify the inclusion of bark beetle dynamics into land surface models. Hence, the objectives of this study are (1) to develop and implement a spatially implicit bark beetle outbreak model in the land surface model ORCHIDEE based on the work by Temperli et al. (2013), and (2) use a simulation experiment to evaluate the performance of this newly added model functionality.

2. Methods and material

2.1. The land surface model ORCHIDEE

95 ORCHIDEE is the land surface model of the IPSL (Institut Pierre Simon Laplace) Earth system model (Krinner et al., 2005; Boucher et al., 2020). ORCHIDEE can, however, also be run off-line as a stand-alone land surface model forced by temperature, humidity, pressure, precipitation, and wind conditions. Unlike the coupled setup, which needs to run on the global scale, the stand-alone configuration can cover any area ranging from a single grid point to the global domain.

100 ORCHIDEE does not enforce any particular spatial resolution. The spatial resolution is an implicit user setting that is determined by the resolution of the climate forcing (or the resolution of the atmospheric model in a coupled



105

configuration). ORCHIDEE can run on any temporal resolution. This apparent flexibility is somewhat restricted as processes are formalized at given time steps: half-hourly (e.g., photosynthesis and energy budget), daily (i.e., net primary production), and annual (i.e., vegetation demographic processes). Hence, meaningful simulations have a temporal resolution of one minute to one hour for the calculation of energy balance, water balance, and photosynthesis.

110

ORCHIDEE is a vegetation distribution model that utilizes meta-classes to describe different types of vegetation. The model includes 13 meta-classes by default, including one class for bare soil, eight classes for various combinations of leaf-type and climate zones of forests, two classes for grasslands, and two classes for croplands. Each meta-class can be further subdivided into an unlimited number of plant functional types (PFTs). The current default setting of ORCHIDEE distinguishes 15 PFTs. Within a single meta-class, various PFTs can be defined based on specific parameters, such as species-specific parameters and age classes. As a simple example, different types of broadleaf temperate forest PFTs, such as beech and oak species, could be simulated using different photosynthetic rates or phenology threshold values.

115

At the beginning of a simulation, each forest PFT in ORCHIDEE contains a monospecific forest stand that is defined by a user-defined but fixed number of diameter classes (three by default). Throughout the simulation, the boundaries of the diameter classes are adjusted to accommodate changes in the stand structure, while the number of classes remains constant. Flexible class boundaries provide a computationally efficient approach to simulate different forest structures. For instance, an even-aged forest is simulated by using a small diameter range between the smallest and largest trees, resulting in all trees belonging to the same stratum. Conversely, an uneven-aged forest is simulated by applying a wide range between diameter classes, such that different classes represent different strata.

120

The model uses allometric relationships to link tree height and crown diameter to tree diameter. Individual tree canopies are not explicitly represented, instead a canopy structure model based on simple geometric forms developed by Haverd et al. (2012) has been included in ORCHIDEE (Naudts et al., 2015). Diameter classes represent trees with different mean diameter and height, which informs the user about the social position of trees within the canopy. Intra-stand competition is based on the basal area of individual trees, which accounts for the fact that trees with a higher basal area occupy dominant positions in the canopy and are therefore more likely to intercept light and thus contribute more to stand-level photosynthesis and biomass growth compared to suppressed trees (Deleuze et al., 2004). If recruitment occurs, diameter classes evolve into cohorts. However, in the absence of recruitment, all diameter classes

125

130

contain trees of the same age. The allocation scheme is based on the pipe model theory (Shinozaki et al., 1964) and its implementation by Sitch et al. (2003); Zaehle and Friend (2010); Zaehle and Dalmonech (2011). According to this scheme, carbon is allocated to different biomass pools (leaves, fine roots, and sapwood) while respecting differences in basal area and tree height between diameter classes as well as longevity and hydraulic conductivity between biomass pools of the same diameter class (Naudts et al., 2015).

135

Individual tree mortality from self-thinning, wind storms, and forest management is explicitly simulated. Other sources of mortality are implicitly accounted for through a so-called constant background mortality rate. Furthermore, age classes (four by default) can be used after land cover change, forest management, and disturbance events to



140 explicitly simulate the regrowth of the forest. Following a land cover change, biomass and soil carbon pools (but not soil water columns) are either merged or split to represent the various outcomes of a land cover change. The ability of ORCHIDEE to simulate dynamic canopy structures (Naudts et al., 2015; Ryder et al., 2016; Chen et al., 2016), a feature essential to simulate both the biogeochemical and biophysical effects of natural and anthropogenic disturbances, is exploited in other parts of the model, i.e., precipitation interception, transpiration, energy budget calculations, the radiation scheme, and the calculation of the absorbed light for photosynthesis.

145 Since revision 7791, mortality from bark beetle outbreaks is now explicitly accounted for and thus conceptually excluded from the so-called environmental background mortality. Subsequently, changes in canopy structure resulting from growth, forest management, land cover changes, wind storms, and bark beetle outbreaks are accounted for in the calculations of the carbon, water, and energy exchanges between the land surface.

150 ORCHIDEE's functionality that is not of direct relevance for this study, e.g., energy budget calculations, soil hydrology, snow phenology, albedo, roughness, photosynthesis, respiration, phenology, land cover changes, product use, and the nitrogen cycle are detailed in (Krinner et al., 2005; Zaehle and Friend, 2010; Naudts et al., 2015; Vuichard et al., 2019)).

2.2. Bark beetle outbreaks in ORCHIDEE

155 2.2.1. Origin of the bark beetle module

Although mortality from windthrow (Chen et al., 2018) and forest management (Naudts et al., 2015; Luyssaert et al., 2018) were already accounted for in ORCHIDEE prior to r7791, insect outbreaks and their interaction with other disturbances were not. The LandClim model (Schumacher et al., 2004) approach and more specifically the bark beetle module developed by Temperli et al. (2013) were adjusted to develop a bark beetle module in ORCHIDEE r7791.

160 LandClim is a spatially explicit stochastic landscape model in which forest dynamics are simulated at a yearly time step for 10–100 km² landscapes consisting of 25 × 25 m patches. Within a patch recruitment, growth, mortality and competition among age cohorts of different tree species are simulated with a gap model (Bugmann, 2001) in response to monthly mean temperature, climatic drought, and light availability. LandClim, for which a detailed description can be found in Schumacher et al., (2004), includes the functionality to simulate the decadal dynamics and consequences

165 of bark beetle outbreaks at the landscape-scale (Temperli et al., 2013). In the LandClim approach, the extent, occurrence and severity of beetle-induced tree mortality are driven by the landscape susceptibility, beetle pressure, and infested tree biomass. While the LandClim beetle module was designed and structured to be generally applicable for northern hemisphere climate-sensitive bark beetle-host systems, it was originally parameterized to represent disturbances by the European spruce bark beetle (*Ips typographus* Linnaeus) in Norway spruce (*Picea abies* Karst.;

170 Temperli et al. 2013).

As ORCHIDEE and LandClim are developed for different purposes, their temporal and spatial scales differ. These differences in model resolution justified adjusting the original model while still following the principles embedded in the LandClim approach. LandClim assesses bark beetle damage at 25 m x 25 m patches and to do so it uses information from other nearby patches as well as landscape characteristics such as slope, aspect and altitude. The susceptibility of

175 a landscape to bark beetle infestations is calculated using multiple factors such as drought-induced tree resistance, age



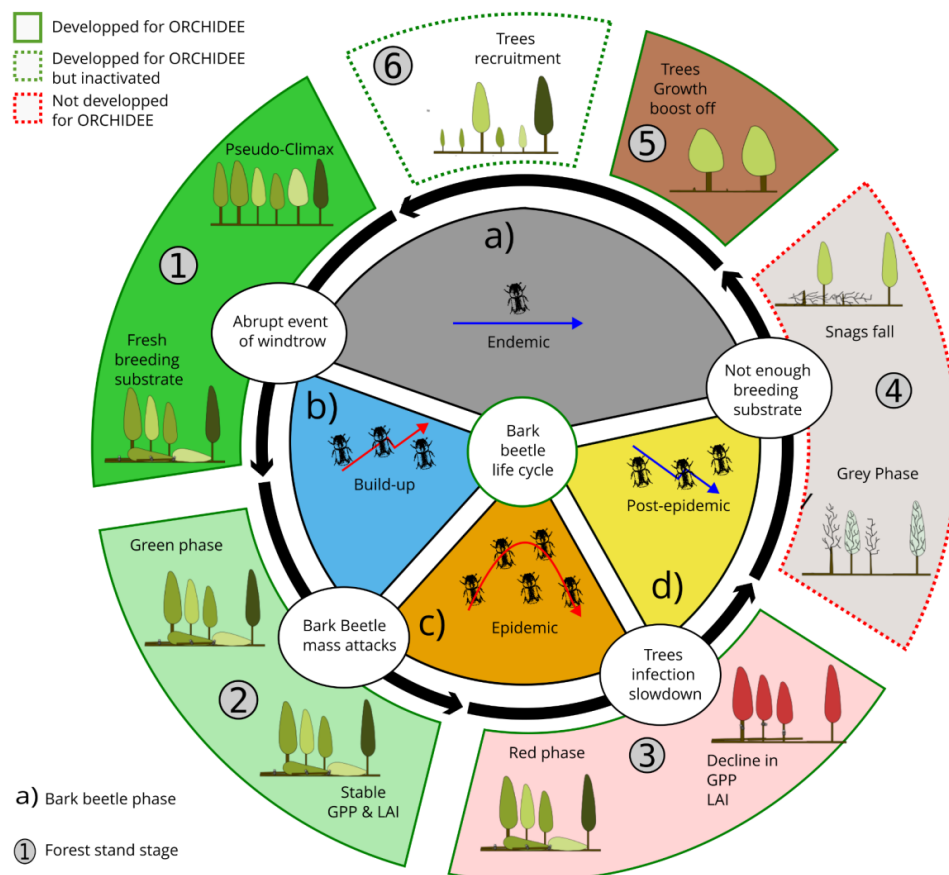
of the oldest spruce cohort, proportion of spruce in the patch's basal area, and windthrow-damaged spruce biomass. These factors, presented as a sigmoidal relationship, range from 0 to 1, indicating no to maximum susceptibility respectively. The susceptibility index for each Norway spruce cohort in a patch is then calculated and used to estimate the biomass of trees killed by bark beetles.

180 Bark beetle pressure is quantified as the potential number of beetles that can infest a patch, calculated considering factors like previous beetle activity, maximum possible spruce biomass that beetles could kill, and a temperature-dependent bark beetle phenology model. This allows the determination of the total infested tree biomass, accounting for stochastic processes with a beta distribution.

185 Finally, the total biomass killed by bark beetles is estimated for each cohort within a patch. The main equations used in this approach, as well as required modifications to account for differences between the LandClim and ORCHIDEE models, are summarized in Table S1.

In ORCHIDEE, however, the simulation unit is about six orders of magnitude larger, i.e., 25 km x 25 km. Hence, a single pixel in ORCHIDEE exceeds the size of an entire landscape in LandClim. Where landscape characteristics in LandClim can be represented by a statistical distribution, the same characteristics in ORCHIDEE are summarized in 190 a single value. These differences between LandClim and ORCHIDEE imply that the original bark beetle module cannot be implemented in ORCHIDEE without adjustments. Hence, the original bark beetle module was modified to obtain a pixel-level model that does not account for the spatial information and statistical distribution of landscape characteristics.

195 In the following we will detail the development of the bark beetle outbreak module into ORCHIDEE by following the forest stand stages and bark beetle outbreak stages introduced in Fig. 1. For clarity, we explain the mechanisms of infestation (section 2.2.2) and mortality (section 2.2.3) separately.



200 **Figure 1: Life cycle of a bark beetle outbreak and subsequent dynamics of a forest stand. The life cycle of an outbreak**
 includes the following stages: a) the “endemic stage” at which the forest stand experiences low bark beetle pressure enabling
 the forest to maintain a pseudo-climax or climax depending on whether the stand is managed or not (shown as stage 1). b)
 The “build-up” stage is characterized by a rapid increase in the bark beetle population due to an event that weakened part
 of the trees but without visible impact on healthy trees (stage 1 & 2). c) During the “epidemic stage” bark beetles are so
 205 numerous that they can successfully attack healthy trees causing a change in leaf colour (stage 2 & 3). d) In the “post-
 epidemic stage” a significant reduction in the bark beetle population occurs due to a lack of substrate for feeding and
 breeding (stage 3 & 4). Stage 4: In the “gray stage” infected trees that retain their leaves and remain standing, gradually
 die turning into so-called snags. Stage 5: in the “ecological transition” stage degradation from wind throws and bark beetles
 result in openings in the canopy reducing-between tree competitions. In Stage 6 bark beetles return to their initial
 210 population level resulting in a new endemic stage during which recruitment may help the forest to reach a (pseudo-)climax
 stage.



2.2.2. Mechanisms of infestation

As in LandCLIM (see table S1), the ORCHIDEE model represents the density of the bark beetle population indirectly through the beetle pressure index (BPI):

$$BPI = Cbp \cdot Si \cdot \frac{(G + Act_{y-1})}{2} \quad (1)$$

The BPI is driven by the number of beetle generations (G) that could occur in the current year, the bark beetle damage from the previous year (Act_{y-1}), and the stand's susceptibility to infestation by bark beetles (Si), which are calculated as an index ranging from 0 to 1:

$$G = \left(1 + e^{-r \cdot (rDD - m)}\right)^{-1} \quad (2)$$

Where r and m are parameters of the logistic function formalizing the relationship with the number of generations (rDD). rDD is calculated as:

$$rDD = \frac{sumTeff}{k} \quad (3)$$

Where $sumTeff$ represents the sum of effective temperatures for bark beetle reproduction in $^{\circ}C \cdot day^{-1}$, while K denotes the thermal sum of degree days for one bark beetle generation in $^{\circ}C \cdot day^{-1}$. rDD can reach up to three or in exceptional cases even four generations, but the index G reaches its maximum value of one when 2.5 or more generations occur in a single growing season. The $sumTeff$ is incremented from January 1st until the diapause of the first generation. In ORCHIDEE, diapause is triggered when daylength exceeds 14.5 hours (e.g., April 27th for France). Each day before the diapause with a daily average temperature above 8°C is accounted for in $sumTeff$. This approach simulates the phenology of bark beetles, which tend to breed earlier when winter and spring are warmer, thus allowing for multiple generations in the same year (Hlásny et al., 2021).

The BPI is also driven by the bark beetle damage index from the previous year (Act_{y-1}):

$$Act_{y-1} = \frac{Bdb_{y-1}}{Bt \cdot Cst} \quad (4)$$

Where Bdb_{year-1} denotes the bark beetle damage from the previous year, Bt is the total biomass of the stand, and Cst is a temporal scaling factor that has to be adjusted depending on the temporal resolution of the bark beetle outbreak module.



255 The stand's susceptibility to infestation by bark beetles (S_i) is the third driver of BPI:

$$S_i = S_{iw} \cdot W_w + S_{ir} \cdot W_r + S_{id} \cdot W_d + S_{is} \cdot W_s \quad (5)$$

260 Where, S_{iw} , S_{ir} , S_{id} , and S_{is} denote the susceptibilities of bark beetles to various environmental factors: breeding substrate (S_{iw}), availability of trees weakened due to water stress (S_{ir}), availability of trees weakened due to inter-tree competition (S_{id}), and prevalence of monospecific stands (S_{is}). Similarly, W_w , W_r , W_d , and W_s represent the weights associated with these susceptibilities. In ORCHIDEE, W_s and W_d are fixed at 0.1. The absolute values for the remaining weights, W_r and W_w , change depending on the stage of the bark beetle outbreak.

265 The transition in the outbreak stage from endemic to epidemic is determined by a risk index, which is computed as $RI = SI * BPI$. If the risk index surpasses the threshold of 0.1 (a value deemed high enough to confidently classify it as a critical threshold), the epidemic flag is switched to 1 and the weights W_r and W_w are computed as:

$$W_r = \left(1 + e^{(r_1 \cdot (S_i \cdot BPI - r_2))}\right)^{-1} \cdot (1 - W_s + W_d) \quad (6)$$

$$W_w = 1 - (W_r + W_s + W_d) \quad (7)$$

270

On the other hand, if the bark beetle outbreak stage is endemic, W_r and W_w are computed as:

$$W_r = 1 - (W_d + W_s); W_w = 0 \quad (8)$$

275 By changing the susceptibility weights between the two stages, ORCHIDEE simulates hysteresis of the drivers that lead to an epidemic and the drivers that allow the forest exit the epidemic stage. Hysteresis in ecology relates to the concept that the path of “recovery” is not the same as the path of “degradation”, often due to complex interactions and feedback loops within the ecosystem (e.g., Staal et al., 2020).

280 The trigger that increases a forest stand's susceptibility to bark beetle infestation is the volume of trees that have recently died. The primary natural source of this woody biomass pool is windstorms. Up until about one year following a windstorm, uprooted and broken stems can be colonized by bark beetles, providing a suitable substrate for breeding and population increase (Nageleisen and Grégoire, 2022). ORCHIDEE formalizes this dependency by using a breeding substrate susceptibility index (S_{iw}):

$$285 \text{ If } S_{iw} < 1, S_{iw} = \frac{Litw}{Bw} / Litt; \text{ Else, } S_{iw} = 1 \quad (9)$$

290 where $Litw$, Bw , and $Litt$ indicate the quantity of breeding substrate for bark beetles, total woody biomass of the stand, and the threshold at which the ratio $Litw/Bw$ is considered maximum, respectively. A windthrow event causes a sudden increase, or pulse, in the breeding substrate in ORCHIDEE, which is employed in computation of the breeding substrate susceptibility index. This substrate becomes unsuitable for beetle breeding after one year, according to



Nageleisen and Grégoire (2022), and is henceforth excluded from the calculation of the breeding substrate susceptibility. This susceptibility index ranges from 0 (indicating no fresh woody biomass available in the litter) to 1 (equivalent to 30% or more of the litter being fresh woody biomass).

In the original formulation of Temperli et al. (2013) the relationship between windthrow and susceptibility was empirical (correlative relationship). In our version, we try to add more realism by introducing the breeding substrate which is a consequence of windthrow and is the real driver of windthrow susceptibility. The threshold (Litt) value of 0.3 was introduced to prevent excess breeding substrate from artificially boosting the bark beetle population, as fresh woody litter does not remain fresh for more than one year. The implication is that more than 30% of new woody litter in one year cannot be exploited by a bark beetle population. In other words, adding more fresh woody litter is thought to have no further impact on the bark beetle population (Hervé Jactel personal communication). As a result, regions or younger forests with a smaller wood volume tend to have a lower threshold than mature forests. However, the susceptibility index (SI) of younger and less dense forests is also limited by susceptibility to interspecific competition. ORCHIDEE determines the susceptibility of forests to infestation using three additional susceptibility indices:

- Susceptibility of weakened trees (Sid). Trees defend themselves against beetle attacks by producing secondary metabolites (Huang et al., 2020). The high carbon and nitrogen costs of these compounds limit their production to periods with environmental conditions favorable for growth (Lieutier, 2002). Trees experiencing extended periods of environmental stress are expected to have less carbon and nitrogen reserves available for defensive substance production, making them more vulnerable to successful bark beetle attacks even at relatively low beetle population densities (Raffa et al., 2008). For this study, the average drought intensity during the last three years is considered, as a proxy of tree health:

$$Sid = \sum_{nac=1}^{ac} (1 + e^{d1 \cdot ((1 - MO_{max_{ac}}) - d2)})^{-1} \cdot Frac_{ac} \quad (10)$$

With,

$$MO_{max_{ac}} = \max(MO, \dots, MO_{n-3}) \quad (11)$$

- Susceptibility due to between-tree competition (Sir). Interspecific competition among trees for limited resources leads to decreased photosynthesis and thus less carbohydrate reserves, resulting in lower investments in defense compounds. In ORCHIDEE, the relative density index (RDI) is used to estimate the average competition between trees at the stand level. At an RDI of 1, the forest is expected to be at its maximum density given the carrying capacity of the site, implying the highest level of competition between trees:

$$Sir = \frac{a1 + (1 - a1)}{(1 + e^{a2 \cdot (RDI_{sp} - a3)})} \quad (12)$$

325



- Susceptibility to forest species purity (Sis). Many forest pests cause more damage in pure forests than in mixed stands (Jactel et al., 2021). *Ips typographus* outbreaks are also more frequent in pure spruce stands (Nardi et al., 2022). Even just a few non-host trees, like deciduous trees, may disrupt the host-searching behavior of dispersing beetles due to the emission of non-host volatile compounds (Zhang and Schlyter, 2004). ORCHIDEE r7791 cannot simulate multi-species stands but does account for landscape-level heterogeneity of forests with different plant functional types. The bark beetle module in ORCHIDEE assumes that within a pixel, the fraction of spruce over other tree species of trees is a proxy for the degree of mixture:

330

$$Sis = (1 + e^{s1 \cdot (sh - s2)})^{-1}, \text{With } Sh_{sp} = \frac{Frac_{sp}}{Frac_{others}} \quad (13)$$

335

Finally, the infested biomass ($Binf$) is calculated as:

$$Binf = Bt \cdot Cst \cdot SI \cdot BPI \quad (14)$$

- 340 Note that the susceptibility of forest to infestation (Si), and the beetle pressure index (BPI) are calculated for the pixel as a whole, despite the existence of multiple age classes.

2.2.3. Mechanisms of mortality

- 345 A tree rarely dies solely from bark beetle damage (except during mass attacks). However, female beetles often carry blue-stain fungi, which colonizes the phloem and sapwood, blocking the water-conducting vessels of the tree. This results in tree death from carbon starvation or desiccation (Nageleisen and Grégoire, 2022). As ORCHIDEE r7791 does not simulate the effects of changes in sapwood conductivity on photosynthesis and the resultant probability of tree mortality, susceptibility due to weakened trees (Sid) and susceptibility due to between-tree competition (Sir) are used as proxies in calculating the fraction of infected trees that eventually die, i.e., the mortality rate ($Siac$):

350

$$Siac = Sir \cdot Wr + Sid \cdot (1 - Wr) \quad (15)$$

Finally, the killed woody biomass (Bdb) is calculated as the product of the actual wood biomass (as a function of the basal area, BA) and the mortality rate.

355

$$Bdb = \sum_{nac}^{ac=1} \frac{Siac + BPI}{2} \cdot Binf \cdot \frac{BA_{ac}}{BA_{sp}} \quad (16)$$

- 360 Mortality happens on the tree-level in ORCHIDEE, and thus the killed biomass must be converted into the number of trees per diameter class. Mortality first affects trees from the largest diameter class (those preferred by bark beetles) before affecting smaller diameter classes until the killed woody biomass (Bdb) has been met. The aboveground and



belowground biomass pools (e.g., leaves, sapwood, heartwood) in the trees killed by bark beetles are then transferred directly into the respective litter pools.

2.2.4. Difference from the original formulation from LANDCLIM

365 The main changes between the model implemented in ORCHIDEE and the original model from Temperli et al., 2013 include various modifications to account for the difference in spatial scale, as ORCHIDEE operates at the landscape rather than a patch. This primarily affected the calculation of the susceptibility. The ORCHIDEE version is also based on dynamic biomass values, as the maximum biomass is not fixed and instead depends on factors like soil fertility, climate, and human management.

370 Further changes were made to account for the different temporal scales in ORCHIDEE and the fact that ORCHIDEE does not distinguish individual species but groups them into plant functional types (PFTs). The model was also adjusted to account for practices like salvage logging and to incorporate different methods of quantifying plant water stress. Finally, the susceptibility of each age class within a pixel was introduced instead of each cohort within a forest patch.

375

2.2.5. Bark beetle development stages

In ORCHIDEE r7791, only two bark beetle development stages are explicitly simulated: endemic and epidemic. Simulated mechanisms of positive and negative feedback on the bark beetle pressure index mimic implicitly two transition stages. Transition stages, referred to as the build-up and post-epidemic stage, were added to the model output as an additional post-processing step in order to facilitate the evaluation and presentation of the simulation results. The thresholds proposed for these transitions affect the figures and subsequent discussion but not the course of the actual simulation as they are only added after the simulations have finished.

380

2.2.5.1. The endemic stage (a)

385 During the endemic stage both the bark beetle population and the number of trees killed are at their lowest values (Fig. 1). At low population densities, beetles can only attack weakened trees or trees that were uprooted or broken within the previous year. In the endemic stage, the susceptibility of a forest mainly depends on the amount of breeding substrate (*Litw*; see table 2). In ORCHIDEE, during the endemic stage bark beetle damage to the forest stand has little impact on the structure and function of the ecosystem. Losses can be considered as background mortality.

Table 2: Definition of the stages used in the study.

Outbreak stages	Stages representing the evolution of the bark beetle population from an endemic to an epidemic situation. There are four stages represented by Latin lower case letters a, b, c, and d representing endemic, build-up, epidemic, and post-epidemic, respectively.
Stand forest stages	Stages representing the health status of a forest stand before, during and after a bark beetle outbreak. There are six stages represented by Arabic numbers from 1 to 6 representing



pseudo-climax, green, red, gray, growth boost, and recruitment, respectively.

390

2.2.5.2. The build-up stage (b)

During the build-up stage, the beetle population is fuelled by an increased availability of breeding substrate that enables the beetle population to grow beyond its endemic size. The build-up stage is a transitory stage during which the population of bark beetles can either return to its endemic stage or evolve into an epidemic stage. In the build-up stage, tree defense mechanisms are activated preventing bark beetles from successfully attacking healthy trees. Consequently, tree canopies remain green and therefore this stage is also known as the green stage (Fig. 1).

395

As the build-up stage is not explicitly represented in ORCHIDEE, we cannot precisely tag the start and the end of the stage. Nonetheless it was estimated during post-processing by considering two thresholds:

400

- The threshold at which the BPI is too high to represent an endemic population. Based on the simulation results, a BPI > 0.13 was selected as the post-processing threshold to mark the end of the endemic stage (Fig. 2).
- The second threshold represents the value of BPI which inevitably results in an epidemic stage. Again, based on the simulation results a BPI > 0.3 will always lead to an epidemic stage (Fig. 2).

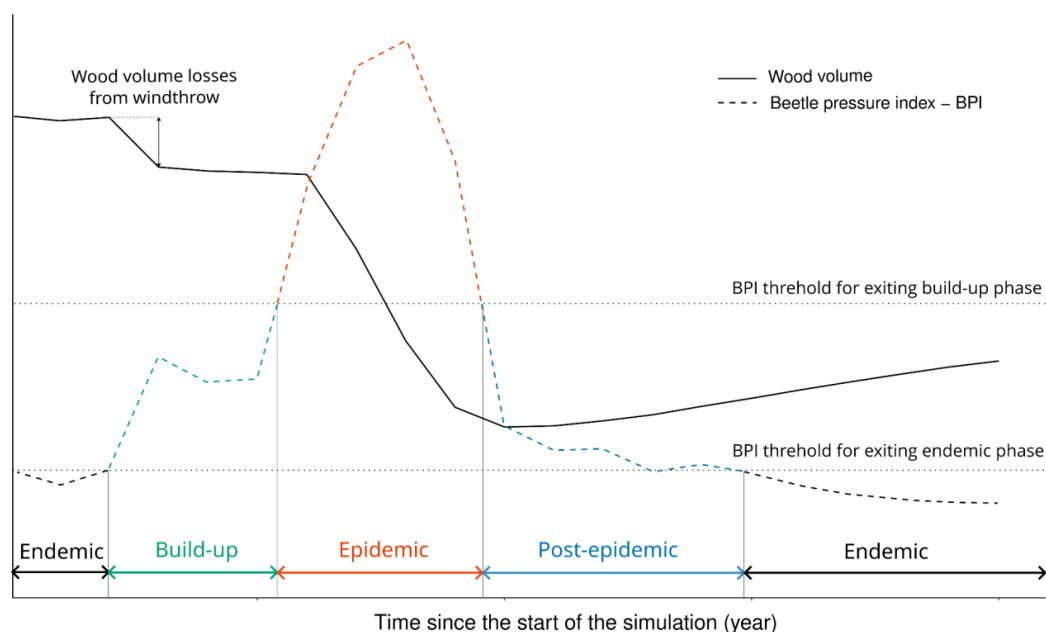


Figure 2: The endemic, build-up (green), epidemic (red), and post-epidemic (blue) stages in the development of a bark beetle outbreak based on synthetic data. The beetle outbreak stages are defined on the basis of the beetle pressure index (unitless) which is a proxy of beetle population size and shown as the dotted line. The full line represents the evolution of wood volume (m³/ha).

405



During the build-up stage, the number of beetle generations and the susceptibility of forest to get infested determine the future of the outbreak. Increasing values for these two drivers will increase bark beetle activity (Act_{year-i}) which can subsequently result in positive feedback on the BPI in the following years leading to an epidemic. When the beetle generations index and the susceptibility of the forest to infestation are not favorable, e.g., cold and wet years, the bark beetles will consume all accessible breeding substrate (Siw) leading to a decrease in both Siw and beetle pressure index.

2.2.5.3. The epidemic stage (c)

The epidemic stage corresponds to the capability of bark beetles to mass attack healthy trees and overrule tree defenses (Biedermann et al., 2019). At this point in the outbreak, all trees are potential targets irrespective of their health. Owing to the widespread mortality of individual trees, the forest dies resulting in a stage also known as the red stage (Fig. 1, stage 3). In order to simulate mass attacks in ORCHIDEE, the weights of two specific susceptibilities (Siw and Sid) in the calculation of the susceptibility index (Si) are different compared to the endemic stage (eq. 6a). In the epidemic stage $Ww=0$ because beetles can access all trees whether healthy or not. Consequently, the weight for Wr is equal to one as it represents the breeding substrate susceptibility accounting for every tree.

Three causes may explain the end of an epidemic: (1) the most likely cause is a high interspecific competition among beetles for breeding substrate when the density of tree hosts is decreasing (decreasing Sir) (Pineau et al., 2017; Komonen et al., 2011), (2) extreme climate events such as heat waves, flood, and frost can abruptly decrease the beetle population (decreasing Sid), and (3) a rarely demonstrated increasing population of beetle predators (Reeve and Turchin, 2002). In ORCHIDEE r7791, the first two causes are represented but the last, i.e., the predators are not represented.

2.2.5.4. The post-epidemic stage (d)

Similar to build-up, the post-epidemic stage is a transitory stage delineated during the post-processing of ORCHIDEE r7791 simulation results. During this stage, the forest is still subject to higher mortality than usual but signs of recovery appear (Hlásny et al., 2021). Recovery may help the forest ecosystem to return to its original state or switch to a new state (different species, change in the forest structure) depending on the intensity and the frequency of the disturbance (Van Meerbeek et al., 2021; Fig. 1).

2.3. Simulation experiments

Eight locations were selected which represent the range of climatic conditions within the distribution area of spruce in Europe (*Picea Abies* Karst L.) as shown in Table 4. Half-hourly weather data from the FLUXNET database (Pastorello et al., 2020) for these locations were used to drive ORCHIDEE. Some of these locations (FON, SOR, HES, COL, WET) are not populated with spruce but all are located within the species distribution. For each location, a pure spruce stand was simulated and the available FLUXNET data was looped to simulate a 100-year period. The study did not investigate the effect of species mixture in the simulation experiments. Other inputs, including soil



texture, pH and soil color were obtained from the USDA map derived from Eswaran et al. (2003), for the corresponding pixel.

Table 4: Climate characteristics of the eight sites used in the gradient underlying our experimental setup. The site acronyms refer to the site names used in the FLUXNET database (Pastorello et al. 2020).

Site (FLUXNET abv.)	Full name	Country	Latitude (°N)	Longitude (°E)	Mean annual temperature (°C)	Min annual temperature (°C)	Mean annual precipitation (mm.y ⁻¹)
HYY	Hyytiälä	Finland	61.8	24.3	3.8	-10.8	522
SOR	Sorø	Danmark	55.5	11.6	8.2	2.7	811
THA	Tharandt	Germany	50.9	13.6	8.2	-3.9	734
WET	Trebon	Czech Republic	49.0	14.8	7.7	-5.2	587
HES	Hesse	France	48.4	7.1	9.5	0.1	653
FON	Fontainebleau	France	48.7	2.8	10.2	-1.1	989
REN	Renon	Italy	46.5	11.4	4.7	-6.3	752
COL	Collelongo	Italy	41.8	13.6	6.3	-3.8	1050



Mean annual net radiation (w.m ⁻²)	42.1	49.4	52.5	68.0	53.7	50.3	67.7	68.3
--	------	------	------	------	------	------	------	------

445

Table 3: Simulated wood volume loss for the different wind speeds prescribed in this study. Wind storms were used as the disruptive event to trigger change in the ecosystem structure. Seven different wind speeds were used in the experimental setup.

Max wind speed (m.s ⁻¹)	19	21	22	23	29	35	40
Relative wood volume loss (%)	0	8	10	12	27	47	>60
Wood volume loss (m ³ . ha ⁻¹)	0	50	70	100	200	300	>300

450

The amount of fresh breeding woody substrate inputs used by the bark beetles to breed was controlled by modifying the maximum wind speed of a windthrow event in ORCHIDEE. Seven wind speeds ranging between 19 m/s and 40 m/s were selected (Table 3). This range is justified by the observation that mean wind speeds below 19 m/s could not trigger a windthrow event in ORCHIDEE (Chen et al., 2018) while for wind speeds exceeding 40 m/s, more than 60% of the trees are uprooted, leaving too few living trees to trigger a bark beetle outbreak within the same pixel.

455

To investigate the impact of windthrow intensity and background climate on bark beetle outbreaks, the study conducted a total of 56 [8 sites x 7 wind speed intensities] simulations as given in table 3. The same 56 simulations were also used to analyze the sensitivity of the carbon balance of spruce forests to windthrow intensity and background climate.

460

Where most land surface models use a turnover time to simulate continuous mortality (Turner et al., 2014; Pugh et al., 2019), ecological reality is better described by abrupt mortality events. An idealized simulation experiment was used to qualify the impact of abrupt mortality on net biome productivity by changing from a framework in which mortality is approximated by a constant background mortality to a framework in which mortality occurs in abrupt, discrete events. To test the impact of a change in mortality framework two versions of ORCHIDEE were compared to create an idealized simulation experiment: (1) a version simulating mortality as a continuous process, labeled "the continuous version", and (2) the version capable of simulating abrupt mortality from windthrow and subsequent bark beetle outbreaks, labeled "the abrupt version". The effect of simulating abrupt mortality was evaluated over 20-, 50-, and 100-year time horizons.

465

The effect of changing the framework of simulating mortality from continuous to abrupt was qualified on the basis of 112 simulations (8 sites x 7 wind speeds x 2 model versions) of 100 years each. The simulations with abrupt mortality were run first. Subsequently, the number of trees killed was quantified and used as a reference value for the continuous mortality set-up. This approach resulted in the same quantities of dead trees at the end of the simulation for both frameworks, which then differed only in the timing of the simulated mortality. This precaution is necessary to avoid

470



comparing two different mortality regimes where the result would mainly be explained by the intensity of the mortality rather than by its underlying mechanisms.

2.4. Quantitative evaluation

475 This study presents a qualitative evaluation, whereas a quantitative evaluation is the topic of an ongoing study. The qualitative evaluation assesses whether the newly developed bark beetle model in ORCHIDEE is capable of reproducing bark beetle outbreak behavior along climate and windthrow gradients. As shown in Fig. 1, a bark beetle outbreak is driven by the beetle population dynamics resulting in structural and functional changes in the forest ecosystem. The length of the development stage of a bark beetle outbreak are not prescribed in ORCHIDEE, but
480 emerge from the implemented processes. The evaluation of the beetle's population dynamics covers the 12 years following a disturbance event. The literature was searched for peer-reviewed papers that present the length of one or several of the outbreak stages. Eleven papers were identified and used in the evaluation (Table 6).

Changes in forest functioning were evaluated through the temporal evolution of the net primary production (NPP) over a 15-year time frame and net biome productivity (NBP) over a 100-year time frame. NBP is defined as the
485 regional net carbon accumulation after considering losses of carbon from fire, harvest, and other episodic disturbances. NBP is a key variable in the carbon cycle of forest ecosystems (Chapin et al., 2006; Galloway and Melillo, 1998) as it integrates photosynthesis, autotrophic, and heterotrophic respiration. In ORCHIDEE, NBP is calculated as proposed in (Chapin et al., 2006)). Changes in net biome productivity are thus the result of changes in photosynthesis, which in turn is driven by changes in leaf area, autotrophic respiration, and heterotrophic respiration. The latter is influenced
490 by the availability of litter inputs, including litter from trees that died from the bark beetle outbreak.

3. Results

3.1. Sensitivity of bark beetles outbreaks to temperature and windthrown intensity.

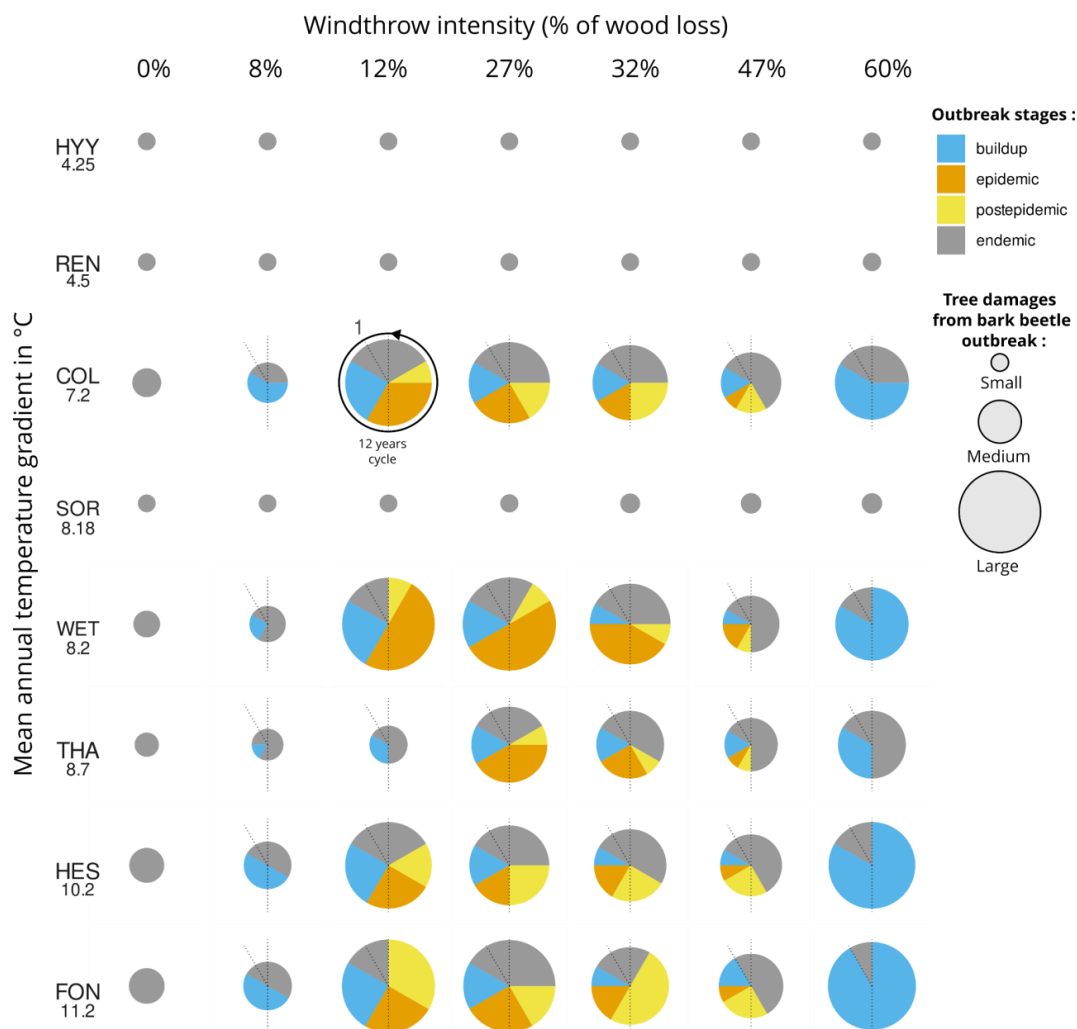


Figure 3: Simulated dynamic of bark beetle outbreaks in spruce forests in the first 20 years after a windthrow event. The criteria used to attribute the simulated beetle population to the different outbreak stages is detailed in table 5. In the left panel an identical and fixed relative wood volume loss from windthrow (i.e., 12%) was applied for each site. The eight sites (Table 4) were used as reference sites for which seven additional simulations were run in order to evaluate the impact of windthrow intensity (outbreak trigger intensity) on the length of the outbreak stages. The simulated relationship between wind speeds and relative wood losses from windthrow are given in Table 3.

495

3.1.1. Back beetle outbreak dynamic along a temperature gradient.

The variation in mean annual temperature across the eight examined locations spanned from a low of 4.3°C in HYY, Finland, to a high of 11.2°C in FON, France, over the simulation period. The hottest sites, FON and HES, witnessed a substantial bark beetle outbreak in ORCHIDEE following a windthrow event, resulting in a minimum of 12% timber loss. In contrast, the coldest sites, HYY and REN, remained unaffected by bark beetles, regardless of the severity of



500 the windthrow event. Interestingly, the four sites with a similar average annual temperature (ranging between 7.2°C and 8.7°C) did not conform to the large-scale temperature gradient that governs bark beetle outbreaks in ORCHIDEE, as was the case in HYY, REN, FON, and COL. For instance, despite having an average annual temperature of 7.2°C, COL experienced an outbreak, while THA (8.7°C) only endured the buildup phase before reverting to the endemic phase with 12% timber loss. Additionally, SOR, which had an average annual temperature of 8.2°C, did not experience
505 any outbreak in the simulations.

Examining the dynamics of net primary production during the outbreak, it's noticeable that warmer sites like FON, HES, and COL recovered more quickly (within 2-3 years) than colder sites (which took 3-5 years) following a disturbance event. This held whether or not the bark beetle population developed into an outbreak (see Fig. 4). The recovery of the fluxes was relatively fast compared to the several decades necessary for the forest structure to recover
510 (result not shown). For locations where no beetle outbreak occurred (i.e., HYY, SOR, REN, as shown in Fig. 3), the recovery was solely from the impact of the windstorm, and these locations returned to their quasi-stable state within 5 to 10 years following the windstorm. At SOR, the climate record contained two storm events within a 5-year period (one that was artificially imposed for the study and one that was naturally present in the climate series), which may have contributed to the longer recovery stage compared to HYY and THA. When considering the total net primary
515 production over a period of 15 years, less productive sites experienced more impact from an outbreak than the more productive sites (Fig. 5).

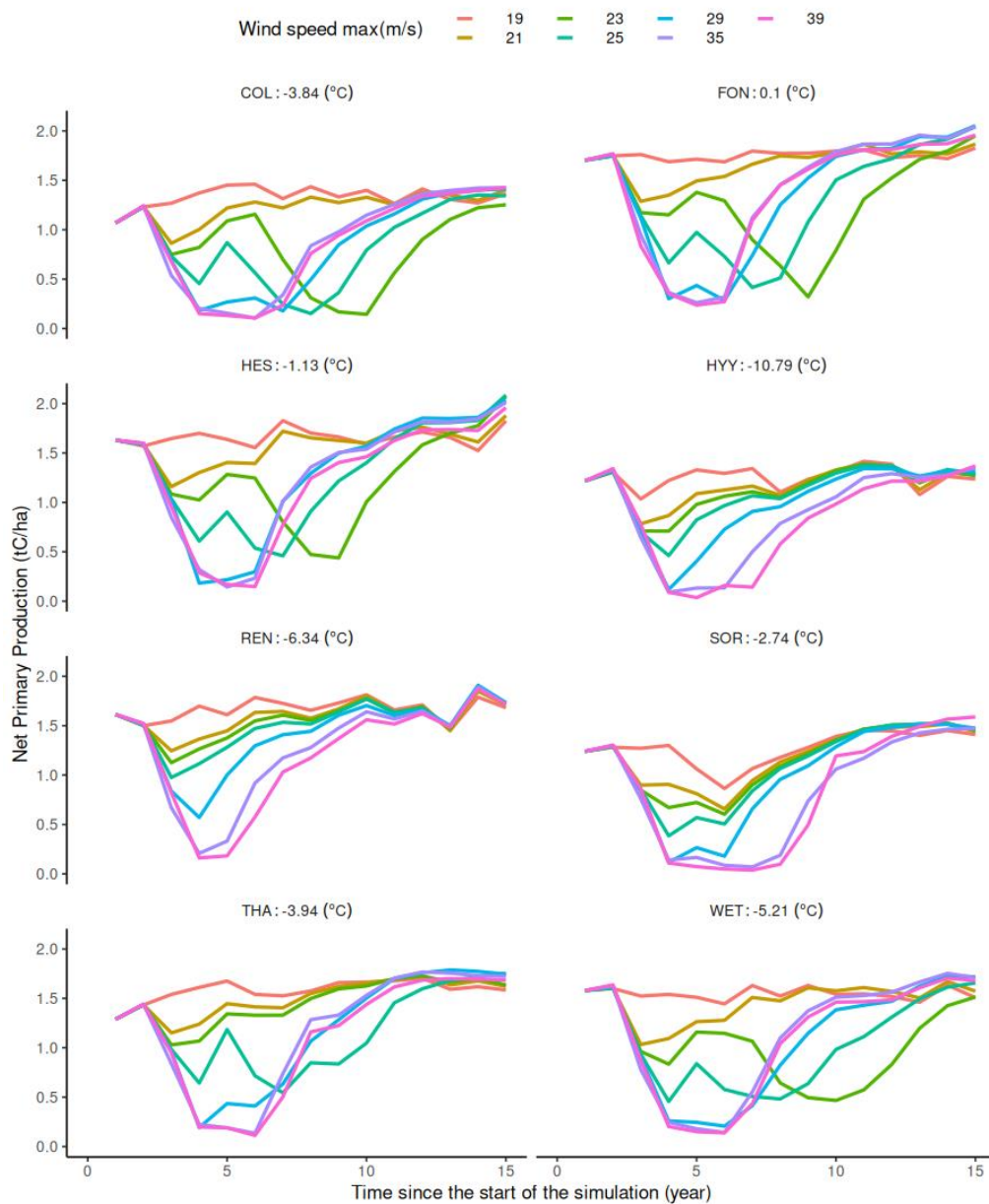


Figure 4: Net primary production for a simulation period of 15 years. At the beginning of year two a windthrow event is forced based on its maximum wind speed (colored line). Each wind speed corresponds to a certain amount of wood loss (see Table 3 for the corresponded value). Each panel represents one of the eight FLUXNET sites studied.



3.1.2. Back beetle outbreak dynamic across windthrow intensity gradient.

520 The ORCHIDEE simulation revealed a consistent correlation between the intensity of windthrow events and the
dynamics of bark beetle outbreaks across all examined locations. In this study, if a windthrow resulted in less than
approximately 12% of timber volume loss, it did not result in an outbreak. The buildup phase, which typically lasted
for three years at a 12% timber loss, reduced to two years at a 27% loss, and further shortened to one to two years at
sites with a 32% loss or more (such as WET, HES, FON). The epidemic phase followed a similar trend, with its
525 duration decreasing from six to three years at a 12% loss, to just one to two years at a 47% loss (Fig. 3). However, at
a 60% timber loss, no epidemic phase was observed. Instead, an extended buildup phase lasting between five and
twelve or more years was simulated. Beyond a 60% loss, the forest density became too low to trigger an outbreak,
even though the vast amount of timber provided by the windthrow maintained the bark beetle population above its
endemic threshold.

530 Analyzing the functional recovery along a gradient of windthrow intensities, it was found that a 12% loss of wood
volume required 13 years to recover, while a loss of 8% required only 5 years (Fig. 4). Interestingly, when considering
the total net primary production over a period of 15 years, it's apparent that the combined impact of windthrow and a
bark beetle outbreak has a greater effect on ecosystem functioning than an equivalent single disturbance event, such
as a windthrow that kills the same overall number of trees (Fig. 5).

535

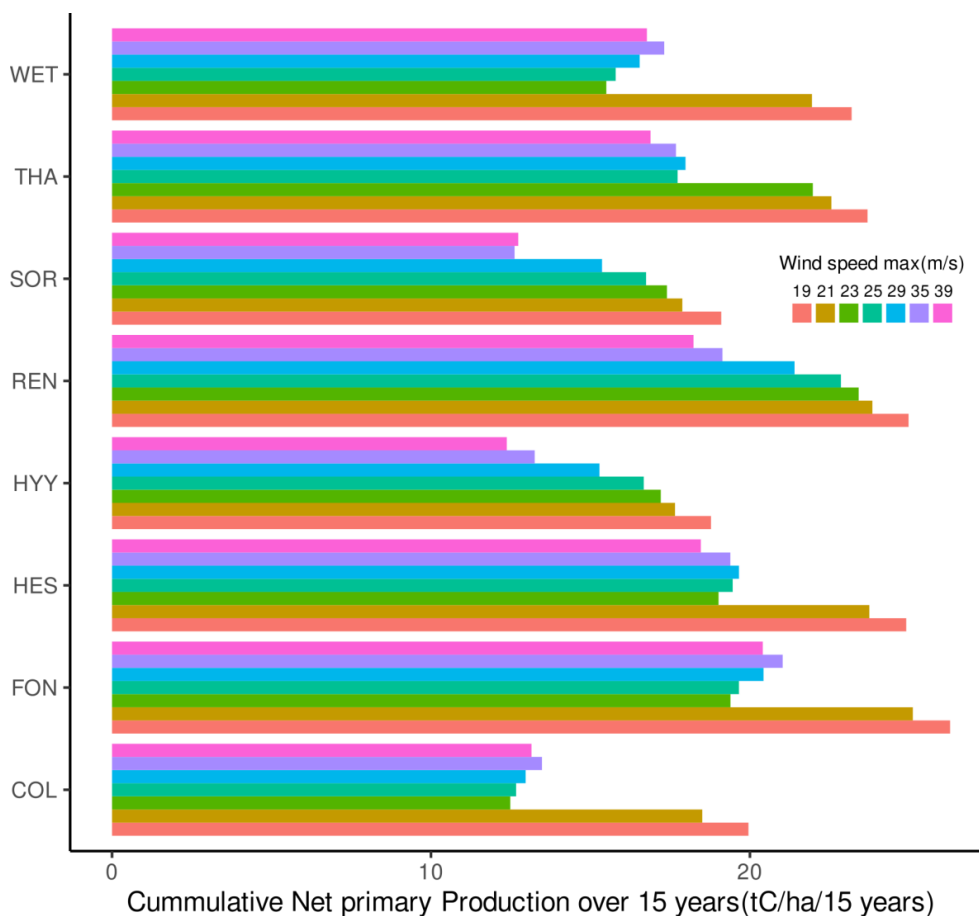


Figure 5: Accumulated net primary production over 15 years. Each group of colored bars represents a FLUXNET site for which seven wind storm intensities have been tested. Higher values mean undisturbed forests and lower values mean highly disturbed forests. See table 3 for the corresponding wood loss % at each max wind speed.

3.2. Comparing simulated and observed bark beetle outbreak dynamics.

When confronting the simulation results with field observations reported in the literature, reasonable agreement was observed in terms of the duration of the four stages of bark beetle outbreak. A comprehensive summary of our findings
540 for each of these four stages is presented in Table 5.

Table 5. Key components of a bark beetle outbreak. We conducted a comprehensive literature review, specifically focusing on peer-reviewed articles that outlined the duration of one or multiple stages of the outbreak. In total, 11 papers were identified and utilized in this evaluation.



Observed elements of a bark beetle outbreak (Fig. 1)	ORCHIDEE behavior
Climax with endemic stage (Fig. 1; outbreak stage a)	
<p>Windthrow provides fresh breeding substrate, thereby increasing bark beetle population (Lausch et al. 2011). Temperature impacts all bark beetle life stages, with higher temperatures facilitating multiple generations in a single year, which in turn drastically increases the bark beetle population (Benz et al. 2005). Cold and wet years decelerate bark beetle breeding (Benz et al. 2005, Nageleisen, 2022).</p>	<p>In colder regions, an increase in temperature following a windthrow event could accelerate the growth of the beetle population and potentially instigate an epidemic situation, as demonstrated in the case of COL (Fig. 3).</p> <p>Conversely, in warmer locations, colder temperatures after a windthrow event could halt the increase in the beetle population, thereby preventing epidemic situations, as seen in the case of THA (Fig. 3).</p> <p>Strong windthrow events resulting in more than 27% damage may lead to a shorter outbreak, as there are fewer living trees available and not all the fresh fallen wood can be utilized by the bark beetles for breeding during the buildup stage (Fig. 3).</p> <p>For weaker windthrow events causing approximately 12% of damage, the likelihood of an epidemic situation will greatly depend on the specific and temporal climatic conditions (Fig. 3).</p>
Green or buildup stage (Fig. 1; outbreak stage b)	
<p>The population of bark beetles expands due to the availability of fresh dead wood biomass. A notable surge in the population of <i>I. typographus</i>, a species of bark beetle, was observed in windthrow areas during the second to third summer following the storm (Wermelinger, 2004).</p>	<p>Based on our simulations, the duration of the buildup stage varied from 1 to 3 years, contingent on the intensity of the windthrow events and the prevailing climate conditions (Fig. 3).</p>
Red or epidemic stage (Fig. 1; outbreak stage c)	
<p>Substantial populations of bark beetles have the capability to launch a mass attack on healthy trees, effectively overcoming their natural defenses (Lieutier et al., 2004, Nageleisen, 2022).</p>	<p>The ORCHIDEE model simulates epidemic stages where all trees with a diameter greater than 20 cm become potential hosts. During these stages, the bark beetle population escalates, reaching levels 6 to 8 times higher than those in the endemic stage (Fig. 2).</p>
<p>Large-scale tree mortality leads to resource scarcity for the bark beetles, subsequently causing a reduction in their population due to intraspecific competition. The duration of the bark beetle epidemic stage ranges from 1 to 5 years, contingent on the severity of the outbreak and the density of the forest (Edburg et al. 2012, Hlásny et al. 2021).</p>	<p>The ORCHIDEE model simulates an epidemic stage lasting between 1 to 6 years, depending on the prevailing climate conditions (Fig 3). A significant decline in the beetle population is observed when the relative stem density drops too low (around 0.4)</p>
<p>The factors that instigate a bark beetle outbreak, such as climate conditions and the availability of fresh dead woody biomass, are different from those that lead to the conclusion of an outbreak, namely resource limitations (Edburg et al. 2012).</p>	<p>The ORCHIDEE model emulates the observed hysteresis, or delay in response, in the dynamics of the beetle population, as outlined in the model description.</p>



Grey or post-epidemic stage (Fig. 1; outbreak stage d)	
<p>The grey stage represents an extended period, spanning years to decades, during which trees die and decompose while still standing, also known as snags (Edburg et al. 2012). During this stage, a disconnection between the soil and ecosystem carbon and nitrogen cycles may be observed (Hlásny et al. 2021).</p>	<p>The ORCHIDEE model simulates logs but not snags. In the model, tree death is instantaneous, with 90% of logs from wind throw and bark beetle damage decomposing within a span of 1 to 3 years (data not shown). This is applicable when logs are lying on the ground. To accurately represent the process in the ORCHIDEE model, snags must be explicitly represented, or the rate of log decomposition must be artificially decreased.</p>
Ecological transition in endemic stage (Fig. 1; outbreak stages 4 to 6)	
<p>In the aftermath of a bark beetle outbreak, which resulted in a 52% reduction in tree numbers, a combination of observational and modeling approaches estimated a recovery period of 25 years (Pfeifer et al. 2011).</p>	<p>Without snag decomposition, the model simulates an extended period of functional recovery, ranging from 5 to 15 years depending on the intensity of the bark beetle outbreak (Fig. 4).</p>
<p>The gradual disappearance of snags tends to favor natural regeneration (Jonášová and Prach, 2004, Carlson et al. 2020).</p>	<p>The ORCHIDEE model does not simulate natural regeneration in this study. This limitation, along with the model's inability to accurately represent snags, could be responsible for its overestimation of the recovery stage.</p>

545

3.3. Continuous vs abrupt mortality

The total net biome production (NBP) was evaluated for each simulation across three different timeframes: 20, 50, and 100 years following a windthrow event. At the 20-year mark, the average accumulated NBP notably differed between the continuous and abrupt mortality frameworks: $2.10 \pm 0.82 \text{ tC}\cdot\text{ha}^{-1}$ for the former, and $-9.73 \pm 10.43 \text{ tC}\cdot\text{ha}^{-1}$ for the latter. These differences were statistically significant (t-test, p-value < 0.001). While forests under the abrupt mortality framework behaved as carbon sources, those under the continuous mortality framework acted as carbon sinks (Fig. 6). Furthermore, the variability in NBP (Fig. 6) demonstrated the broad temperature gradient in Europe and indicated that despite many locations potentially acting as sources under the abrupt mortality framework, some may transition to carbon sinks within the first 20 years following a disturbance.

555 When considering the 50-year horizon, the difference between the two frameworks decreased. The net biome productions were 6.00 ± 2.09 and $0.77 \pm 6.15 \text{ tC}\cdot\text{ha}^{-1}$ for the continuous and abrupt mortality frameworks, respectively. The difference in sink strength was statistically significant (t-test, p-value = 0.001), with the NBP in the abrupt framework approaching carbon neutrality. However, the variability of responses depending on climatic conditions remained pronounced under the abrupt framework in comparison to the continuous one. Some locations under the abrupt mortality framework transitioned from carbon sources to carbon sinks under the continuous mortality framework (Fig. 6).

560 At the 100-year mark, the average accumulated NBP for the abrupt and continuous frameworks became indistinguishable (t-test, p-value = 0.55), with values of 20.98 ± 7.90 and $22.90 \pm 9.77 \text{ tC}\cdot\text{ha}^{-1}$, respectively.

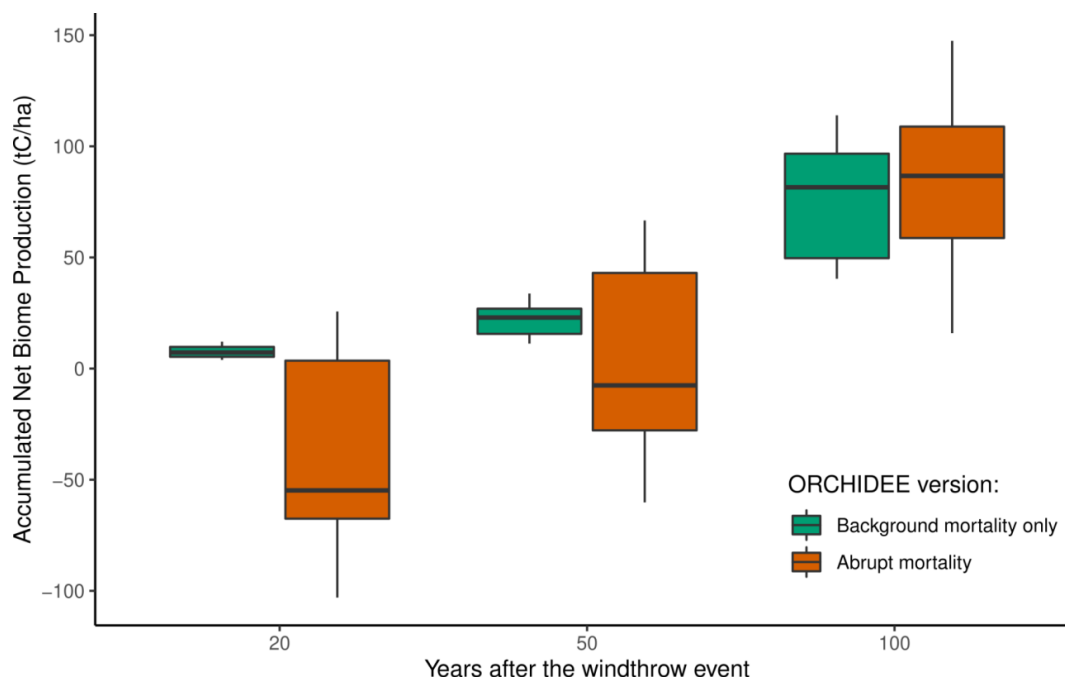


Figure 6: Difference in cumulative net biome production at three discrete time horizons (i.e., 20, 50 and 100 years) between a continuous (green) and abrupt (orange) mortality framework. Note that in the continuous mortality framework the mortality rate was adjusted to obtain a similar number of trees killed after 100 years as in the abrupt mortality framework. The variation of each boxplot arises due to different locations and prescribed storm intensities. Each boxplot displays the median value (thick horizontal line), the quartile range (box border), and the 95% confidence interval (vertical line).

565 4. Discussion

4.1. Simulating the dynamics of bark beetle outbreaks and their interaction with windthrow

Given the large-scale nature of the ORCHIDEE model we opted to start with a qualitative evaluation of the bark beetle outbreak functionality rather than focusing the evaluation on matching observed damage volumes at specific case studies. Such an approach is thought to reduce the risk of overfitting the model to specific site conditions (Abramowitz et al., 2008). Qualitative evaluation enables improving the realism of the bark beetle model in ORCHIDEE without reducing its generality (Levins, 1966). The side-by-side comparison of the observed stages in a bark beetle outbreak and model behavior by ORCHIDEE (Table 6) show the ability of ORCHIDEE to simulate the dynamics of cascading disturbances. Even if some of the simulated dynamics may rarely occur in reality, the model formulation has demonstrated its capability to simulate a broad range of disturbance dynamics. The variation in the outbreak dynamics and the response of the outbreak to its main drivers (Fig. 3) give confidence in the ability of ORCHIDEE to simulate various outbreak scenarios observed around the temperate and boreal zones under changing climate conditions.

4.2. Emerging property from interacting disturbances



580

While this study hasn't provided a precise quantification of the impact of incorporating abrupt mortality versus a fixed continuous background mortality, it consistently demonstrated that the impact of abrupt mortality can vary across locations and over time, i.e., ecosystem functions, such as carbon storage, are affected by natural disasters like pest outbreaks, having significant impacts on short-to-mid-term carbon balance estimates.

585

The experiments also highlighted that the legacy effects of disturbances can endure for decades, even in a simplified representation of forest ecosystems such as ORCHIDEE, where the recovery might be too fast due to the absence of snags or too slow due to the absence of recruitment (Senf et al., 2019).

590

In the model wind speeds of less than 20 m.s⁻¹ weren't powerful enough to uproot or break trees (Fig. 4). The ability to simulate resistance as an emerging property is evident from Fig. 4 for locations SOR, REN, and HYY, where no bark beetle outbreaks were observed following a windthrow. However, in all simulated locations that couldn't resist a bark beetle outbreak, the forest was resilient and ecosystem functions were restored to the level from before the wind throw. The elasticity of, e.g., the carbon sink capacity ranged from 1 to 10 years. This elasticity is in line with current observational evidence from Millar and Stephenson (2015) who found very little evidence of ecosystem shifts due to natural disturbances in forests. Finally, after the disturbance and the recovery of vegetation structure, the ecosystems simulated by ORCHIDEE showed persistence, i.e. the ability to continue along their initial developmental path.

595

4.3. Are cascading disturbances important for carbon balance estimates?

600

The integration of abrupt mortality events instead of a fixed continuous mortality calculation has significantly complicated the ORCHIDEE model. However, does this increased realism offer any new insights into carbon balance estimates? The experiment suggests that over a century-long timeframe, the net biome production, which was used to estimate carbon balance, remains consistent regardless of if a continuous or abrupt framework is used. This further corroborates the model's ability to reach the same state (Fig. 6). The time needed for both frameworks to convergence implies that after a single disturbance or a cascade of disturbances, the forest experiences a prolonged growth spurt that compensates for the growth deficit during the disturbance event.

605

The experiment, however, did not consider fluctuations in the recurrence of disturbances. Considering the significant impact of disturbance legacy on carbon dynamics, it's plausible that a recurrence interval of less than the recovery period could trigger a tipping point, reducing the carbon sequestration beyond the 100-year horizon. In extreme cases, forest ecosystems might even collapse, although this was not simulated in the current experiments nor documented in the recent review by Millar and Stephenson (2015).

610

On the other hand, between 20 to 50 years, the commonly adopted continuous mortality model tends to overestimate the carbon sink capacity of forests compared to conditions with abrupt mortality events. Since most policy recommendations target these shorter timeframes (e.g. Green Deal for Europe, 2023; Paris Agreement | CCNUCC, 2023) they should rely on model simulations incorporating an abrupt mortality framework to avoid overestimation of the sink capacity of forest.

Moreover, this study emphasizes the significance of initializing the model with an accurate depiction of the forest's state. The state of the forest greatly influences the carbon assimilation rate. Integrating an abrupt mortality framework



615 into the ORCHIDEE model may help to enhance the accuracy and robustness of our carbon balance estimates over
short, medium, and long-term periods.

4.4. Bark beetle outbreak models shortcomings

620 The bark beetle outbreak module developed in this study builds upon the strengths of the previously established
LandClim model, though it also inherited some of its limitations.

One notable shortcoming is the submodule for beetle phenology, which is an empirical model making use of
accumulated degrees. Since the model's conception a decade ago, Europe's climate has undergone substantial changes,
primarily manifested in warmer winters and springs (European State of the Climate | Copernicus, 2023). Because of
these changes the chances have increased for two or even more bark beetle generations within a calendar year (Hlásny
625 et al., 2021). These changes call for an update of the beetle's phenology model to align with these more recent
observations (Ogris et al., 2019).

Another issue is the model's consideration of drought. As outlined in the method section, drought is treated as an
exacerbating factor, rather than a primary trigger as is the case for windthrow. This understanding was accurate a
decade ago (Temperli et al., 2013); however, emerging evidence increasingly suggests that drought events may indeed
630 trigger bark beetle outbreaks across Europe (Netherer et al., 2015; Nardi et al., 2022). Consequently, this extreme
drought as a trigger should be incorporated in a future revision of ORCHIDEE's bark beetle outbreak module.

5. Outlook

This study simulated how windthrow interacts with bark beetle infestations in unmanaged forests. Future research will
635 incorporate additional interactions, such as: the interplay between droughts, storms, and bark beetles; storms, bark
beetles, and fires; as well as forest management, storms, and bark beetles.

The bark beetle outbreak module could also be enhanced by simulating: (a) standing dead trees (or snags), which
would help account for differences in wood decomposition between snags and logs (Angers et al., 2012; Storaunet
and Rolstad, 2004), (b) the migration of bark beetles to neighboring locations, which becomes significant to account
640 for in a model that operates at spatial resolutions below approximately 10 kilometers, (c) the recruitment of trees,
which would enable the simulation of ecosystem shifts (see section 4.2), and (d) an up-to-date beetle phenology
module which accounts for the recent change in their behavior induced by climate change.

This research provides an initial qualitative assessment of a new model feature. However, the application of the model
necessitates an evaluation of the simulations against observations of cascading disturbances at the regional scale,
645 which is the topic of an ongoing study.

6. Conclusion

The integration of a bark beetle outbreak in interaction with other natural disturbance such as windthrow into the
ORCHIDEE land surface model has resulted in a broader range of disturbance dynamics and has demonstrated
650 ORCHIDEE's capacity to simulate various disturbance interaction scenarios under different climatic conditions.
Incorporating abrupt mortality events instead of a fixed continuous mortality calculation provided new insights into



carbon balance estimates. The study showed that the continuous mortality framework, which is commonly used in the land-surface modeling community, tends to overestimate the carbon sink capacity of forests in the 20-to-50-year range in ecosystems under high disturbance pressure, compared to scenarios with abrupt mortality events.

655 Apart from these advances, the study revealed possible shortcomings in the bark beetle outbreak model including the need to update the beetle's phenology model to reflect recent climate changes, and the need to consider extreme drought as a trigger for bark beetle outbreaks in line with emerging evidence. Looking ahead, future work will further develop the capability of ORCHIDEE to simulate interacting disturbances such as the interplay between extreme droughts, storms, and bark beetles, and between storms, bark beetles, and fires.

660

7. Code availability

- R script and data are available at:

<https://doi.org/10.5281/zenodo.8004954>

ORCHIDEE rev 7791 code is also available from:

665 https://forge.ipsl.jussieu.fr/orchidee/wiki/GroupActivities/CodeAvailabilityPublication/ORCHIDEE_gmd-2023-05

8. Data availability

- The FLUXNET climate forcing data are available at:

670 <https://fluxnet.org/>

- The simulation results use in this study are available at:

<https://doi.org/10.5281/zenodo.8107315>

9. Author contribution

675 G. Marie, S. Luyssaert designed the experiments and G. Marie conducted them. Following discussions with H. Jactel, G. Petter and M. Cailleret, G. Marie developed the bark beetles model code and performed the simulations. J. Jeong integrated the wind damage and bark beetle modules with each other. G. Marie, J. Jeong, V. Bastrikov, J. Ghattas, B. Guenet, A.S. Lansø, M.J. McGrath, K. Naudts, A. Valade, C. Yue, and S. Luyssaert, contributed to the development, parameterization and evaluation of the ORCHIDEE revision used in this study. G. Marie, J. Jeong, 680 and S. Luyssaert prepared the manuscript with contributions from all co-authors.

10. Competing interests

No competing interest

685 11. Acknowledgements

GM was funded by MSCF (CLIMPRO) and ADEME (DIPROG). SL and KN were funded by Horizon 2020, HoliSoils (SEP-210673589) and Horizon Europe INFORMA (101060309). JJ was funded by Horizon 2020, HoliSoils (SEP-210673589). BG was funded by Horizon 2020, HoliSoils (SEP-210673589). GP acknowledges funding by the Swiss National Science Foundation (SNF 163250). ASL was funded by Horizon 2020, Crescendo (641816). C.Y. was funded



690 by the National Science Foundation of China (U20A2090 and 41971132). MJM was supported by the European
Commission, Horizon 2020 Framework Programme (VERIFY, grant no. 776810) and the European Union's Horizon
2020 research and innovation programme under Grant Agreement No. 958927 (CoCO2). AV acknowledges funding
by Agropolis Fondation (2101-048). The Textual AI - Open AI GPT4 (<https://chat.openai.com/>) has been used for
language editing at an early stage of manuscript preparation.

695

12. References

- Abramowitz, G., Leuning, R., Clark, M., and Pitman, A.: Evaluating the Performance of Land Surface Models, *J. Clim.*, 21, 5468–5481, <https://doi.org/10.1175/2008JCLI2378.1>, 2008.
- 700 Allen, C. D., Breshears, D. D., and McDowell, N. G.: On underestimation of global vulnerability to tree mortality
and forest die-off from hotter drought in the Anthropocene, *Ecosphere*, 6, art129, <https://doi.org/10.1890/ES15-00203.1>, 2015.
- Andrus, R. A., Hart, S. J., and Veblen, T. T.: Forest recovery following synchronous outbreaks of spruce and
705 western balsam bark beetle is slowed by ungulate browsing, *Ecology*, 101, e02998,
<https://doi.org/10.1002/ecy.2998>, 2020.
- Angers, V. A., Bergeron, Y., and Drapeau, P.: Morphological attributes and snag classification of four North
American boreal tree species: Relationships with time since death and wood density, *For. Ecol. Manag.*, 263, 138–
710 147, <https://doi.org/10.1016/j.foreco.2011.09.004>, 2012.
- Un pacte vert pour l'Europe: https://commission.europa.eu/strategy-and-policy/priorities-2019-2024/european-green-deal_fr, last access: 2 June 2023.
- 715 European State of the Climate | Copernicus: <https://climate.copernicus.eu/ESOTC>, last access: 30 May 2023.
- L'Accord de Paris | CCNUCC: <https://unfccc.int/fr/a-propos-des-ndcs/l-accord-de-paris>, last access: 2 June 2023.
- Bentz, B. J., Régnière, J., Fettig, C. J., Hansen, E. M., Hayes, J. L., Hicke, J. A., Kelsey, R. G., Negrón, J. F., and
720 Seybold, S. J.: Climate Change and Bark Beetles of the Western United States and Canada: Direct and Indirect
Effects, *BioScience*, 60, 602–613, <https://doi.org/10.1525/bio.2010.60.8.6>, 2010.
- Biedermann, P. H. W., Müller, J., Grégoire, J.-C., Gruppe, A., Hagge, J., Hammerbacher, A., Hofstetter, R. W.,
Kandasamy, D., Kolarik, M., Kostovcik, M., Krokene, P., Sallé, A., Six, D. L., Turrini, T., Vanderpool, D.,
725 Wingfield, M. J., and Bässler, C.: Bark Beetle Population Dynamics in the Anthropocene: Challenges and Solutions,
Trends Ecol. Evol., 34, 914–924, <https://doi.org/10.1016/j.tree.2019.06.002>, 2019.
- Boucher, O., Servonnat, J., Albright, A. L., Aumont, O., Balkanski, Y., Bastrikov, V., Bekki, S., Bonnet, R., Bony,
S., Bopp, L., Braconnot, P., Brockmann, P., Cadule, P., Caubel, A., Cheruy, F., Codron, F., Cozic, A., Cugnet, D.,
730 D'Andrea, F., Davini, P., Laverigne, C. de, Denvil, S., Deshayes, J., Devilliers, M., Ducharne, A., Dufresne, J.-L.,
Dupont, E., Éthé, C., Fairhead, L., Falletti, L., Flavoni, S., Foujols, M.-A., Gardoll, S., Gastineau, G., Ghattas, J.,
Grandpeix, J.-Y., Guenet, B., Guez, L., E., Guilyardi, E., Guimberteau, M., Hauglustaine, D., Hourdin, F., Idelkadi,
A., Joussaume, S., Kageyama, M., Khodri, M., Krinner, G., Lebas, N., Levvasseur, G., Lévy, C., Li, L., Lott, F.,
Lurton, T., Luyssaert, S., Madec, G., Madeleine, J.-B., Maignan, F., Marchand, M., Marti, O., Mellul, L.,
735 Meurdesoif, Y., Mignot, J., Musat, I., Ottlé, C., Peylin, P., Planton, Y., Polcher, J., Rio, C., Rochetin, N., Rousset,
C., Sepulchre, P., Sima, A., Swingedouw, D., Thiéblemont, R., Traore, A. K., Vancoppenolle, M., Vial, J., Vialard,
J., Viovy, N., and Vuichard, N.: Presentation and Evaluation of the IPSL-CM6A-LR Climate Model, *J. Adv. Model.
Earth Syst.*, 12, e2019MS002010, <https://doi.org/10.1029/2019MS002010>, 2020.
- 740 Bugmann, H.: A Review of Forest Gap Models, *Clim. Change*, 51, 259–305,
<https://doi.org/10.1023/A:1012525626267>, 2001.



- 745 Buma, B.: Disturbance interactions: characterization, prediction, and the potential for cascading effects, *Ecosphere*, 6, art70, <https://doi.org/10.1890/ES15-00058.1>, 2015.
- Chapin, F. S., Woodwell, G. M., Randerson, J. T., Rastetter, E. B., Lovett, G. M., Baldocchi, D. D., Clark, D. A., Harmon, M. E., Schimel, D. S., Valentini, R., Wirth, C., Aber, J. D., Cole, J. J., Goulden, M. L., Harden, J. W., Heimann, M., Howarth, R. W., Matson, P. A., McGuire, A. D., Melillo, J. M., Mooney, H. A., Neff, J. C., Houghton, R. A., Pace, M. L., Ryan, M. G., Running, S. W., Sala, O. E., Schlesinger, W. H., and Schulze, E.-D.: Reconciling Carbon-cycle Concepts, Terminology, and Methods, *Ecosystems*, 9, 1041–1050, <https://doi.org/10.1007/s10021-005-0105-7>, 2006.
- 755 Chen, Y., Ryder, J., Bastrikov, V., McGrath, M. J., Naudts, K., Otto, J., Otlé, C., Peylin, P., Polcher, J., Valade, A., Black, A., Elbers, J. A., Moors, E., Foken, T., van Gorsel, E., Haverd, V., Heinesch, B., Tiedemann, F., Knohl, A., Launiainen, S., Loustau, D., Ogée, J., Vessala, T., and Luysaert, S.: Evaluating the performance of land surface model ORCHIDEE-CAN v1.0 on water and energy flux estimation with a single- and multi-layer energy budget scheme, *Geosci. Model Dev.*, 9, 2951–2972, <https://doi.org/10.5194/gmd-9-2951-2016>, 2016.
- 760 Chen, Y.-Y., Gardiner, B., Pasztor, F., Blennow, K., Ryder, J., Valade, A., Naudts, K., Otto, J., McGrath, M. J., Planque, C., and Luysaert, S.: Simulating damage for wind storms in the land surface model ORCHIDEE-CAN (revision 4262), *Geosci. Model Dev.*, 11, 771–791, <https://doi.org/10.5194/gmd-11-771-2018>, 2018.
- 765 Ciais, P., Reichstein, M., Viovy, N., Granier, A., Ogée, J., Allard, V., Aubinet, M., Buchmann, N., Bernhofer, C., Carrara, A., Chevallier, F., De Noblet, N., Friend, A. D., Friedlingstein, P., Grünwald, T., Heinesch, B., Keronen, P., Knohl, A., Krinner, G., Loustau, D., Manca, G., Matteucci, G., Miglietta, F., Ourcival, J. M., Papale, D., Pilegaard, K., Rambal, S., Seufert, G., Soussana, J. F., Sanz, M. J., Schulze, E. D., Vesala, T., and Valentini, R.: Europe-wide reduction in primary productivity caused by the heat and drought in 2003, *Nature*, 437, 529–533, <https://doi.org/10.1038/nature03972>, 2005.
- 770 Cox, P. M., Betts, R. A., Jones, C. D., Spall, S. A., and Totterdell, I. J.: Acceleration of global warming due to carbon-cycle feedbacks in a coupled climate model, *Nature*, 408, 184–187, <https://doi.org/10.1038/35041539>, 2000.
- 775 Deleuze, C., Pain, O., Dhôte, J.-F., and Hervé, J.-C.: A flexible radial increment model for individual trees in pure even-aged stands, *Ann. For. Sci.*, 61, 327–335, <https://doi.org/10.1051/forest:2004026>, 2004.
- Eswaran, H., Beinroth, F. H., and Reich, P. F.: A Global Assessment of Land Quality, Chapters, 111–132, 2003.
- 780 Friedlingstein, P., Cox, P., Betts, R., Bopp, L., Bloh, W. von, Brovkin, V., Cadule, P., Doney, S., Eby, M., Fung, I., Bala, G., John, J., Jones, C., Joos, F., Kato, T., Kawamiya, M., Knorr, W., Lindsay, K., Matthews, H. D., Raddatz, T., Rayner, P., Reick, C., Roeckner, E., Schnitzler, K.-G., Schnur, R., Strassmann, K., Weaver, A. J., Yoshikawa, C., and Zeng, N.: Climate–Carbon Cycle Feedback Analysis: Results from the C4MIP Model Intercomparison, *J. Clim.*, 19, 3337–3353, <https://doi.org/10.1175/JCLI3800.1>, 2006.
- 785 Haverd, V., Lovell, J. L., Cuntz, M., Jupp, D. L. B., Newnham, G. J., and Sea, W.: The Canopy Semi-analytic Pgap And Radiative Transfer (CanSPART) model: Formulation and application, *Agric. For. Meteorol.*, 160, 14–35, <https://doi.org/10.1016/j.agrformet.2012.01.018>, 2012.
- 790 Hicke, J. A., Allen, C. D., Desai, A. R., Dietze, M. C., Hall, R. J., Hogg, E. H., Kashian, D. M., Moore, D., Raffa, K. F., Sturrock, R. N., and Vogelmann, J.: Effects of biotic disturbances on forest carbon cycling in the United States and Canada., <https://doi.org/10.1111/j.1365-2486.2011.02543.x>, 2012.
- 795 Hlásny, T., König, L., Krokene, P., Lindner, M., Montagné-Huck, C., Müller, J., Qin, H., Raffa, K. F., Schelhaas, M.-J., Svoboda, M., Viiri, H., and Seidl, R.: Bark Beetle Outbreaks in Europe: State of Knowledge and Ways Forward for Management, *Curr. For. Rep.*, 7, 138–165, <https://doi.org/10.1007/s40725-021-00142-x>, 2021.
- Huang, J., Kautz, M., Trowbridge, A. M., Hammerbacher, A., Raffa, K. F., Adams, H. D., Goodsman, D. W., Xu, C., Meddens, A. J. H., Kandasamy, D., Gershenson, J., Seidl, R., and Hartmann, H.: Tree defence and bark beetles



- in a drying world: carbon partitioning, functioning and modelling, *New Phytol.*, 225, 26–36,
https://doi.org/10.1111/nph.16173, 2020.
- 800 Jactel, H., Moreira, X., and Castagneyrol, B.: Tree Diversity and Forest Resistance to Insect Pests: Patterns, Mechanisms, and Prospects, *Annu. Rev. Entomol.*, 66, 277–296, https://doi.org/10.1146/annurev-ento-041720-075234, 2021.
- 805 Kautz, M., Anthoni, P., Meddens, A. J. H., Pugh, T. A. M., and Arneith, A.: Simulating the recent impacts of multiple biotic disturbances on forest carbon cycling across the United States, *Glob. Change Biol.*, 24, 2079–2092, https://doi.org/10.1111/gcb.13974, 2018.
- 810 Komonen, A., Schroeder, L. M., and Weslien, J.: *Ips typographus* population development after a severe storm in a nature reserve in southern Sweden, *J. Appl. Entomol.*, 135, 132–141, https://doi.org/10.1111/j.1439-0418.2010.01520.x, 2011.
- 815 Krinner, G., Viovy, N., de Noblet-Ducoudré, N., Ogée, J., Polcher, J., Friedlingstein, P., Ciais, P., Sitch, S., and Prentice, I. C.: A dynamic global vegetation model for studies of the coupled atmosphere-biosphere system: DVGM FOR COUPLED CLIMATE STUDIES, *Glob. Biogeochem. Cycles*, 19, https://doi.org/10.1029/2003GB002199, 2005.
- 820 Kurz, W. A., Dymond, C. C., Stinson, G., Rampley, G. J., Neilson, E. T., Carroll, A. L., Ebata, T., and Safranyik, L.: Mountain pine beetle and forest carbon feedback to climate change, *Nature*, 452, 987–990, https://doi.org/10.1038/nature06777, 2008.
- Lasslop, G., Thonicke, K., and Kloster, S.: SPITFIRE within the MPI Earth system model: Model development and evaluation, *J. Adv. Model. Earth Syst.*, 6, 740–755, https://doi.org/10.1002/2013MS000284, 2014.
- 825 Levins, R.: The Strategy of Model Building in Population Biology, *Am. Sci.*, 54, 421–431, 1966.
- Lieutier, F.: Mechanisms of Resistance in Conifers and Bark beetle Attack Strategies, in: Mechanisms and Deployment of Resistance in Trees to Insects, edited by: Wagner, M. R., Clancy, K. M., Lieutier, F., and Paine, T. D., Springer Netherlands, Dordrecht, 31–77, https://doi.org/10.1007/0-306-47596-0_2, 2002.
- 830 Luysaert, S., Marie, G., Valade, A., Chen, Y.-Y., Njakou Djomo, S., Ryder, J., Otto, J., Naudts, K., Lansø, A. S., Ghattas, J., and McGrath, M. J.: Trade-offs in using European forests to meet climate objectives, *Nature*, 562, 259–262, https://doi.org/10.1038/s41586-018-0577-1, 2018.
- 835 Mezei, P., Jakuš, R., Pennerstorfer, J., Havašová, M., Škvarenina, J., Ferenčík, J., Slivinský, J., Bičárová, S., Bilčík, D., Blaženec, M., and Netherer, S.: Storms, temperature maxima and the Eurasian spruce bark beetle *Ips typographus*—An infernal trio in Norway spruce forests of the Central European High Tatra Mountains, *Agric. For. Meteorol.*, 242, 85–95, https://doi.org/10.1016/j.agrformet.2017.04.004, 2017.
- 840 Migliavacca, M., Dosio, A., Kloster, S., Ward, D. S., Camia, A., Houborg, R., Houston Durrant, T., Khabarov, N., Krasovskii, A. A., San Miguel-Ayanz, J., and Cescatti, A.: Modeling burned area in Europe with the Community Land Model, *J. Geophys. Res. Biogeosciences*, 118, 265–279, https://doi.org/10.1002/jgrg.20026, 2013.
- 845 Migliavacca, M., Musavi, T., Mahecha, M. D., Nelson, J. A., Knauer, J., Baldocchi, D. D., Perez-Priego, O., Christiansen, R., Peters, J., Anderson, K., Bahn, M., Black, T. A., Blanken, P. D., Bonal, D., Buchmann, N., Caldararu, S., Carrara, A., Carvalhais, N., Cescatti, A., Chen, J., Cleverly, J., Cremonese, E., Desai, A. R., El-Madany, T. S., Farella, M. M., Fernández-Martínez, M., Filippa, G., Forkel, M., Galvagno, M., Gomasasca, U., Gough, C. M., Göckede, M., Ibrom, A., Ikawa, H., Janssens, I. A., Jung, M., Kattge, J., Keenan, T. F., Knohl, A., Kobayashi, H., Kraemer, G., Law, B. E., Liddell, M. J., Ma, X., Mammarella, I., Martini, D., Macfarlane, C., Matteucci, G., Montagnani, L., Pabon-Moreno, D. E., Panigada, C., Papale, D., Pendall, E., Penuelas, J., Phillips, R. P., Reich, P. B., Rossini, M., Rotenberg, E., Scott, R. L., Stahl, C., Weber, U., Wohlfahrt, G., Wolf, S., Wright, I. J., Yakir, D., Zaehle, S., and Reichstein, M.: The three major axes of terrestrial ecosystem function, *Nature*, 598, 468–



- 472, <https://doi.org/10.1038/s41586-021-03939-9>, 2021.
- 855 Millar, C. I. and Stephenson, N. L.: Temperate forest health in an era of emerging megadisturbance, *Science*, 349, 823–826, <https://doi.org/10.1126/science.aaa9933>, 2015.
- 860 Nageleisen, L.-M. and Grégoire, J.-C.: Une vie de typographe : point des connaissances sur la biologie d'*Ips typographus* (Linnaeus 1758), *Rev. For. Fr.*, 73, 479–498, <https://doi.org/10.20870/revforfr.2021.5565>, 2022.
- Nardi, D., Jactel, H., Pagot, E., Samalens, J., and Marini, L.: Drought and stand susceptibility to attacks by the European spruce bark beetle: A remote sensing approach, *Agric. For. Entomol.*, afe.12536, <https://doi.org/10.1111/afe.12536>, 2022.
- 865 Naudts, K., Ryder, J., McGrath, M. J., Otto, J., Chen, Y., Valade, A., Bellasen, V., Berhongaray, G., Bönisch, G., Campioli, M., Ghattas, J., De Groot, T., Haverd, V., Kattge, J., MacBean, N., Maignan, F., Merilä, P., Penuelas, J., Peylin, P., Pinty, B., Pretzsch, H., Schulze, E. D., Solyga, D., Vuichard, N., Yan, Y., and Luysaert, S.: A vertically discretised canopy description for ORCHIDEE (SVN r2290) and the modifications to the energy, water and carbon fluxes, *Geosci. Model Dev.*, 8, 2035–2065, <https://doi.org/10.5194/gmd-8-2035-2015>, 2015.
- 870 Netherer, S., Matthews, B., Katzensteiner, K., Blackwell, E., Henschke, P., Hietz, P., Pennerstorfer, J., Rosner, S., Kikuta, S., Schume, H., and Schopf, A.: Do water-limiting conditions predispose Norway spruce to bark beetle attack?, *New Phytol.*, 205, 1128–1141, <https://doi.org/10.1111/nph.13166>, 2015.
- 875 Ogris, N., Ferlan, M., Hauptman, T., Pavlin, R., Kavčič, A., Jurc, M., and de Groot, M.: RITY – A phenology model of *Ips typographus* as a tool for optimization of its monitoring, *Ecol. Model.*, 410, 108775, <https://doi.org/10.1016/j.ecolmodel.2019.108775>, 2019.
- 880 Pastorello, G., Trotta, C., Canfora, E., Chu, H., Christianson, D., Cheah, Y.-W., Poindexter, C., Chen, J., Elbashandy, A., Humphrey, M., Isaac, P., Polidori, D., Reichstein, M., Ribeca, A., van Ingen, C., Vuichard, N., Zhang, L., Amiro, B., Ammann, C., Arain, M. A., Ardö, J., Arkebauer, T., Arndt, S. K., Arriga, N., Aubinet, M., Aurela, M., Baldocchi, D., Barr, A., Beamesderfer, E., Marchesini, L. B., Bergeron, O., Beringer, J., Bernhofer, C., Berveiller, D., Billesbach, D., Black, T. A., Blanken, P. D., Bohrer, G., Boike, J., Bolstad, P. V., Bonal, D.,
- 885 Bonnefond, J.-M., Bowling, D. R., Bracho, R., Brodeur, J., Brümmer, C., Buchmann, N., Burbank, B., Burns, S. P., Buysse, P., Cale, P., Cavagna, M., Cellier, P., Chen, S., Chini, I., Christensen, T. R., Cleverly, J., Collalti, A., Consalvo, C., Cook, B. D., Cook, D., Coursolle, C., Cremonese, E., Curtis, P. S., D'Andrea, E., da Rocha, H., Dai, X., Davis, K. J., Cinti, B. D., Grandcourt, A. de Ligne, A. D., De Oliveira, R. C., Delpierre, N., Desai, A. R., Di Bella, C. M., Tommasi, P. di, Dolman, H., Domingo, F., Dong, G., Dore, S., Duce, P., Dufrêne, E., Dunn, A.,
- 890 Dušek, J., Eamus, D., Eichelmann, U., ElKhidir, H. A. M., Eugster, W., Ewenz, C. M., Ewers, B., Famulari, D., Fares, S., Feigenwinter, I., Feitz, A., Fensholt, R., Filippa, G., Fischer, M., Frank, J., Galvagno, M., et al.: The FLUXNET2015 dataset and the ONEFlux processing pipeline for eddy covariance data, *Sci. Data*, 7, 225, <https://doi.org/10.1038/s41597-020-0534-3>, 2020.
- 895 Pasztor, F., Matulla, C., Rammer, W., and Lexer, M. J.: Drivers of the bark beetle disturbance regime in Alpine forests in Austria, *For. Ecol. Manag.*, 318, 349–358, <https://doi.org/10.1016/j.foreco.2014.01.044>, 2014.
- Pineau, X., Bourguignon, M., Jactel, H., Lieutier, F., and Sallé, A.: Pyrrhic victory for bark beetles: Successful standing tree colonization triggers strong intraspecific competition for offspring of *Ips sexdentatus*, *For. Ecol. Manag.*, 399, 188–196, <https://doi.org/10.1016/j.foreco.2017.05.044>, 2017.
- 900 Pörtner, H.-O., Roberts, D. C., Tignor, M. M. B., Poloczanska, E. S., Mintenbeck, K., Alegría, A., Craig, M., Langsdorf, S., Lössche, S., Möller, V., Okem, A., and Rama, B. (Eds.): *Climate Change 2022: Impacts, Adaptation and Vulnerability. Contribution of Working Group II to the Sixth Assessment Report of the Intergovernmental Panel on Climate Change.*, 2022.
- 905 Pugh, T. A. M., Lindeskog, M., Smith, B., Poulter, B., Arneth, A., Haverd, V., and Calle, L.: Role of forest regrowth in global carbon sink dynamics, *Proc. Natl. Acad. Sci.*, 116, 4382–4387, <https://doi.org/10.1073/pnas.1810512116>, 2019.



- 910 Quillet, A., Peng, C., and Garneau, M.: Toward dynamic global vegetation models for simulating vegetation–climate interactions and feedbacks: recent developments, limitations, and future challenges, *Environ. Rev.*, 18, 333–353, <https://doi.org/10.1139/A10-016>, 2010.
- 915 Raffa, K. F., Aukema, B. H., Bentz, B. J., Carroll, A. L., Hicke, J. A., Turner, M. G., and Romme, W. H.: Cross-scale Drivers of Natural Disturbances Prone to Anthropogenic Amplification: The Dynamics of Bark Beetle Eruptions, *BioScience*, 58, 501–517, <https://doi.org/10.1641/B580607>, 2008.
- 920 Reeve, J. D. and Turchin, P.: Evidence for Predator-Prey Cycles in a Bark Beetle, in: *Population Cycles: The Case for Trophic Interactions*, edited by: Berryman, A., Oxford University Press, 0, <https://doi.org/10.1093/oso/9780195140989.003.0009>, 2002.
- 925 Ryder, J., Polcher, J., Peylin, P., Ottlé, C., Chen, Y., van Gorsel, E., Haverd, V., McGrath, M. J., Naudts, K., Otto, J., Valade, A., and Luyssaert, S.: A multi-layer land surface energy budget model for implicit coupling with global atmospheric simulations, *Geosci. Model Dev.*, 9, 223–245, <https://doi.org/10.5194/gmd-9-223-2016>, 2016.
- 930 Schumacher, S., Bugmann, H., and Mladenoff, D. J.: Improving the formulation of tree growth and succession in a spatially explicit landscape model, *Ecol. Model.*, 180, 175–194, <https://doi.org/10.1016/j.ecolmodel.2003.12.055>, 2004.
- 935 Seidl, R., Fernandes, P. M., Fonseca, T. F., Gillet, F., Jönsson, A. M., Merganičová, K., Netherer, S., Arpaci, A., Bontemps, J.-D., Bugmann, H., González-Olabarria, J. R., Lasch, P., Meredieu, C., Moreira, F., Schelhaas, M.-J., and Mohren, F.: Modelling natural disturbances in forest ecosystems: a review, *Ecol. Model.*, 222, 903–924, <https://doi.org/10.1016/j.ecolmodel.2010.09.040>, 2011.
- Seidl, R., Schelhaas, M.-J., Rammer, W., and Verkerk, P. J.: Increasing forest disturbances in Europe and their impact on carbon storage, *Nat. Clim. Change*, 4, 806–810, <https://doi.org/10.1038/nclimate2318>, 2014.
- 940 Seidl, R., Thom, D., Kautz, M., Martin-Benito, D., Peltoniemi, M., Vacchiano, G., Wild, J., Ascoli, D., Petr, M., Honkaniemi, J., Lexer, M. J., Trotsiuk, V., Mairota, P., Svoboda, M., Fabrika, M., Nagel, T. A., and Reyer, C. P. O.: Forest disturbances under climate change, *Nat. Clim. Change*, 7, 395–402, <https://doi.org/10.1038/nclimate3303>, 2017.
- 945 Seidl, R., Klöner, G., Rammer, W., Essl, F., Moreno, A., Neumann, M., and Dullinger, S.: Invasive alien pests threaten the carbon stored in Europe’s forests, *Nat. Commun.*, 9, 1626, <https://doi.org/10.1038/s41467-018-04096-w>, 2018.
- 950 Senf, C., Müller, J., and Seidl, R.: Post-disturbance recovery of forest cover and tree height differ with management in Central Europe, *Landsc. Ecol.*, 34, 2837–2850, <https://doi.org/10.1007/s10980-019-00921-9>, 2019.
- SHINOZAKI, K., YODA, K., HOZUMI, K., and KIRA, T.: A QUANTITATIVE ANALYSIS OF PLANT FORM-THE PIPE MODEL THEORY : I.BASIC ANALYSES, 1964.
- 955 Sitch, S., Smith, B., Prentice, I. C., Arneth, A., Bondeau, A., Cramer, W., Kaplan, J. O., Levis, S., Lucht, W., Sykes, M. T., Thonicke, K., and Venevsky, S.: Evaluation of ecosystem dynamics, plant geography and terrestrial carbon cycling in the LPJ dynamic global vegetation model, *Glob. Change Biol.*, 9, 161–185, <https://doi.org/10.1046/j.1365-2486.2003.00569.x>, 2003.
- 960 Staal, A., Fetzer, I., Wang-Erlandsson, L., Bosmans, J. H. C., Dekker, S. C., van Nes, E. H., Rockström, J., and Tuinenburg, O. A.: Hysteresis of tropical forests in the 21st century, *Nat. Commun.*, 11, 4978, <https://doi.org/10.1038/s41467-020-18728-7>, 2020.
- 965 Storaunet, K. O. and Rolstad, J.: How long do Norway spruce snags stand? Evaluating four estimation methods, *Can. J. For. Res.*, 34, 376–383, <https://doi.org/10.1139/x03-248>, 2004.



- Temperli, C., Bugmann, H., and Elkin, C.: Cross-scale interactions among bark beetles, climate change, and wind disturbances: a landscape modeling approach, *Ecol. Monogr.*, 83, 383–402, <https://doi.org/10.1890/12-1503.1>, 2013.
- 970 Thurner, M., Beer, C., Santoro, M., Carvalhais, N., Wutzler, T., Schepaschenko, D., Shvidenko, A., Kompter, E., Ahrens, B., Levick, S. R., and Schmuilius, C.: Carbon stock and density of northern boreal and temperate forests, *Glob. Ecol. Biogeogr.*, 23, 297–310, <https://doi.org/10.1111/geb.12125>, 2014.
- 975 Van Meerbeek, K., Jucker, T., and Svenning, J.-C.: Unifying the concepts of stability and resilience in ecology, *J. Ecol.*, 109, 3114–3132, <https://doi.org/10.1111/1365-2745.13651>, 2021.
- 980 Vuichard, N., Messina, P., Luyssaert, S., Guenet, B., Zaehle, S., Ghattas, J., Bastrikov, V., and Peylin, P.: Accounting for carbon and nitrogen interactions in the global terrestrial ecosystem model ORCHIDEE (trunk version, rev 4999): multi-scale evaluation of gross primary production, *Geosci. Model Dev.*, 12, 4751–4779, <https://doi.org/10.5194/gmd-12-4751-2019>, 2019.
- 985 Yao, Y., Joetzjer, E., Ciais, P., Viovy, N., Cresto Aleina, F., Chave, J., Sack, L., Bartlett, M., Meir, P., Fisher, R., and Luyssaert, S.: Forest fluxes and mortality response to drought: model description (ORCHIDEE-CAN-NHA r7236) and evaluation at the Caxiuana drought experiment, *Geosci. Model Dev.*, 15, 7809–7833, <https://doi.org/10.5194/gmd-15-7809-2022>, 2022.
- 990 Yue, C., Ciais, P., Cadule, P., Thonicke, K., Archibald, S., Poulter, B., Hao, W. M., Hantson, S., Mouillot, F., Friedlingstein, P., Maignan, F., and Viovy, N.: Modelling the role of fires in the terrestrial carbon balance by incorporating SPITFIRE into the global vegetation model ORCHIDEE – Part 1: simulating historical global burned area and fire regimes, *Geosci. Model Dev.*, 7, 2747–2767, <https://doi.org/10.5194/gmd-7-2747-2014>, 2014.
- 995 Zaehle, S. and Dalmonech, D.: Carbon–nitrogen interactions on land at global scales: current understanding in modelling climate biosphere feedbacks, *Curr. Opin. Environ. Sustain.*, 3, 311–320, <https://doi.org/10.1016/j.cosust.2011.08.008>, 2011.
- 1000 Zaehle, S. and Friend, A. D.: Carbon and nitrogen cycle dynamics in the O-CN land surface model: 1. Model description, site-scale evaluation, and sensitivity to parameter estimates, *Glob. Biogeochem. Cycles*, 24, <https://doi.org/10.1029/2009GB003521>, 2010.
- 1005 Zhang, Q.-H. and Schlyter, F.: Olfactory recognition and behavioural avoidance of angiosperm nonhost volatiles by conifer-inhabiting bark beetles, *Agric. For. Entomol.*, 6, 1–20, <https://doi.org/10.1111/j.1461-9555.2004.00202.x>, 2004.
- Zscheischler, J., Westra, S., van den Hurk, B. J. J. M., Seneviratne, S. I., Ward, P. J., Pitman, A., AghaKouchak, A., Bresch, D. N., Leonard, M., Wahl, T., and Zhang, X.: Future climate risk from compound events, *Nat. Clim. Change*, 8, 469–477, <https://doi.org/10.1038/s41558-018-0156-3>, 2018.